AD-A132 571 DONOR BEHAVIOR IN HIGH-PURITY EPITAXIAL INP(U) 1/1
WASHINGTON UNIV ST LOUIS MO SEMICONDUCTOR RESEARCH LAB
C M WOLFE ET AL. 02 OCT 80 64345-25 N00173-78-C-0431
UNCLASSIFIED F/G 20/12 NL

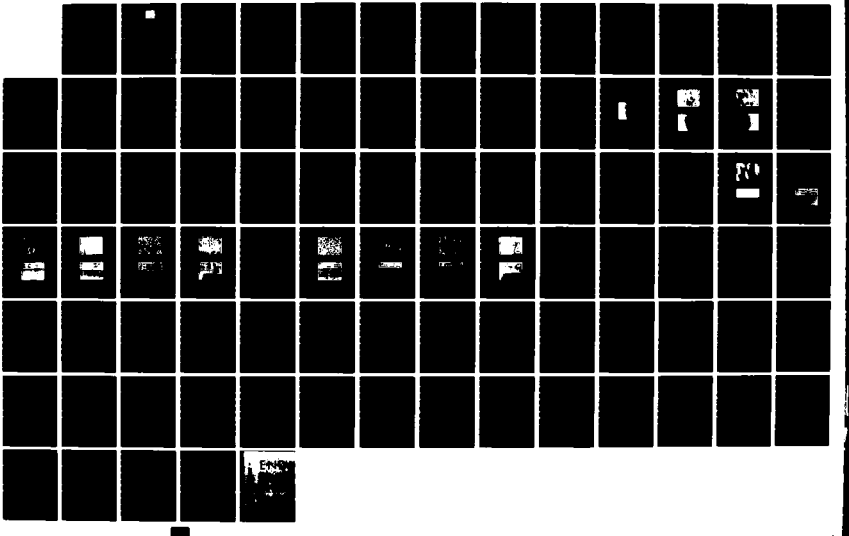

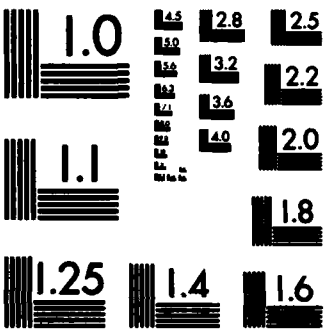

MICROCOPY RESOLUTION TEST CHART
NATIONAL BUREAU OF STANDARDS-1963-A

AD A132571

WASHINGTON UNIVERSITY

SCHOOL OF ENGINEERING AND APPLIED SCIENCE

FINAL TECHNICAL REPORT
No. 64345-25

DONOR BEHAVIOR IN HIGH-PURITY EPITAXIAL InP

2 October 1980
by
Semiconductor Research Laboratory
Box 1127
Washington University
Saint Louis, Missouri 63130
For
Naval Research Laboratory
Code 5220
Washington, DC 20375

Contract No. N00173-78-C-0431

1 June 1978 - 30 June 1980

APPROVED FOR PUBLIC RELEASE
DISTRIBUTION UNLIMITED

DTIC FILE COPY

SEP 1 6 1983

H

83 09 16 126

Unclassified

SECURITY CLASSIFICATION OF THIS PAGE (When Data Entered)

REPORT DOCUMENTATION PAGE		READ INSTRUCTIONS BEFORE COMPLETING FORM
1. REPORT NUMBER	2. GOVT ACCESSION NO. AD-A132 571	3. RECIPIENT'S CATALOG NUMBER
4. TITLE (and Subtitle) Donor Behavior in High-Purity Epitaxial InP		5. TYPE OF REPORT & PERIOD COVERED Final 1 June 1978-30-June 1980
		6. PERFORMING ORG. REPORT NUMBER 64345-25
7. AUTHOR(s) C.M. Wolfe R.T. Green		8. CONTRACT OR GRANT NUMBER(s) N00173-78-C-0431
9. PERFORMING ORGANIZATION NAME AND ADDRESS Semiconductor Research Laboratory Box 1127 Washington University, St.Louis,Mo.63130		10. PROGRAM ELEMENT, PROJECT, TASK AREA & WORK UNIT NUMBERS
11. CONTROLLING OFFICE NAME AND ADDRESS Naval Research Laboratory Code 5220 Washington, DC 20375		12. REPORT DATE 2 Oct 1980
		13. NUMBER OF PAGES 82
14. MONITORING AGENCY NAME & ADDRESS(if different from Controlling Office)		15. SECURITY CLASS. (of this report) Unclassified
		15a. DECLASSIFICATION/DOWNGRADING SCHEDULE

16. DISTRIBUTION STATEMENT (of this Report)

~~The United States Government is authorized to reproduce and distribute this report for Governmental purposes.~~

APPROVED FOR PUBLIC RELEASE
DISTRIBUTION UNLIMITED

17. DISTRIBUTION STATEMENT (of the abstract entered in Block 20, if different from Report)

18. SUPPLEMENTARY NOTES

19. KEY WORDS (Continue on reverse side if necessary and identify by block number)

InP, epitaxy, impurities

DTIC COPY INSPECTED 2

Accession For
NTIS GRA&I
DTIC TAB
Unannounced
Justification
By
Distribution/
Availability Codes
Dist Avail and/or Special
A

20. ABSTRACT (Continue on reverse side if necessary and identify by block number)

The paper presents the results of research undertaken to develop a technology for the improved growth of high-purity, epitaxial InP using the H_2-In-PCl_3 process. A VPE reactor was fabricated and a general reactor model was developed. Based upon early growth runs and application of the reactor model, modifications were made in the standard growth procedures to obtain much higher purity.

DD FORM 1 JAN 73 1473 EDITION OF 1 NOV 65 IS OBSOLETE

Unclassified

SECURITY CLASSIFICATION OF THIS PAGE (When Data Entered)

TABLE OF CONTENTS

No.		Page
1.	Introduction	1
2.	Reaction Equations	2
3.	Apparatus	4
	3.1 Reactor Design	4
	3.2 Growth Parameter Control	9
4.	Reactor Operation	14
	4.1 Source Materials	14
	4.2 Reactor Maintenance	14
	4.3 Growth Procedures	16
	4.3.1 Sample Preparation	16
	4.3.2 Thermal Cycling	18
	4.3.3 Melt Saturation	22
	4.3.4 Growth Procedure	24
5.	Epitaxial Layer Evaluation	29
	5.1 Surface and Interface Characterization	29
	5.1.1 Techniques	29
	5.1.2 Results	30
	5.2 Electrical Characterization	41
	5.2.1 Techniques	41
	5.2.2 Results	47
6.	Reactor Model	56
	6.1 Generalized Reactor Design	57
	6.2 Impurity Incorporation	58
	6.3 Incorporation Function Development	62
	6.3.1 Incorporation Function Statement	63
	6.3.2 Complications	66
7.	Impurity Incorporation Model Application	69
	7.1 General Trends	71
	7.2 Optimum Growth Parameters	72
	7.3 Reacting Species Identification	73

TABLE OF CONTENTS
(Continued)

No.		Page
8.	Conclusions	78
9.	Bibliography	81

1. INTRODUCTION

Recent interest in InP for use in optical and microwave devices has prompted the need for producing high-purity epitaxial InP reproducibly. The object of this paper is to provide a technology for the production of high-purity InP using the PCl_3-In-H_2 process for growing epitaxial InP from the vapor phase. The approach used in developing the technology consists of fabricating a reactor (designated reactor D) similar to vapor phase systems described in the literature, amassing a large amount of data resulting from growth runs performed under various growth conditions for different crystal orientations, and then fitting the data to a reactor model so an optimum set of growth parameters may be chosen to achieve the highest purity. The reactor model shall be derived independently of specific reactor design to insure generality.

2. REACTION EQUATIONS

As with similar chloride systems used by other researchers [1-6], the dominant transport and deposition mechanism is characterized by three reactions. When the PCl_3 enters the hot reaction tube the PCl_3 dissociates and in the presence of H_2 reacts to form P_4 and HCl with the stoichiometry:

$$4PCl_3 + 6H_2 \xrightarrow{T'^{\circ}C} P_4 + 12HCl. \qquad (1)$$

With the presence of elemental indium in contact with the gas flow there occurs a reaction between the indium and P_4:

$$4In + P_4 \xrightarrow{T^{\circ}C} 4InP. \qquad (2)$$

This reaction will dominate the stoichiometric composition of the gas flow downstream of the indium source by depleting P_4 from the stream until the indium is saturated with phosphorus and a solid InP crust is formed which provides a barrier between the gas stream and the indium. This is the melt saturation reaction. The primary reaction responsible for transport and deposition is given by:

$$4InP + 4HCl \underset{(T-100)^{\circ}C}{\overset{T^{\circ}C}{\rightleftharpoons}} 4InCl + P_4 + 2H_2, \qquad (3)$$

where the reaction proceeding from left to right indicates the reaction of HCl with the InP crust to provide the

*The numbers in parentheses in the text indicate references in the Bibliography.

mechanism of phosphorus and indium transport in the system. The reverse reaction which takes place at a temperature approximately 100°C lower than the indium source temperature provides the InP deposition reaction. The reaction equations given above are those dominant for an indium source temperature of 750°C and a deposition temperature of 650°C for a reactor operating at or very near equilibrium. It should be emphasized that departure from equilibrium conditions or change in reactor temperature may destroy the usefulness of these reactions and require modification to include transport due to chlorides of indium other than the mono-chloride as well as phosphorous transport due to P_2. Another failing of the given equations is its neglect of the gas stream reaction with the reactor walls which has been shown to be of major importance at elevated reactor temperatures [5,7].

The usefulness of the reaction equations does not lie in their ability to accurately predict quantitatively the deposition of InP but rather as criteria for evaluating reactor performance as compared with some ideal equilibrium system.

3. APPARATUS

The system described in this section (Reactor D) is the reactor used for all growth experiments.

3.1 REACTOR DESIGN

In Reactor D, provisions were made for the input of argon and ultra high purity (UHP) H_2 into the system. The UHP H_2 was obtained using a palladium diffusion cell and was used as the carrier gas for the system's reaction processes. The high purity argon was used as a flush to provide a non-reactive environment within the system during reactor maintenance. Controls were included so that each gas could be introduced into the system by way of single input line.

Input to the reactor was a single line to the PCl_3 bubbler/containment vessel. The PCl_3 bubbler was constructed entirely of pyrex and consisted of a U-tube with valved input and output. The U-tube had a much larger diameter on the output side and a long length of coiled tubing on the input side to insure thermal equilibrium between the gas flow and its environment. A valved bypass line shunting the gas flow from the input side of the bubbler to the output side was also present so a gas flow could be maintained in the reactor at all times. The shunt line was designed in such a way as to constantly flush the region around each of the containment valves to reduce contamination of the PCl_3 from the atmosphere over long periods of

time. Connection of the bubbler assembly to the reaction tube was accomplished using a solve-seal joint (teflon sleeve and O-ring fitting) with silicone vacuum grease used for lubrication. The solve-seal joint was removed far enough from the furnace to reduce the problems associated with repeated heating and cooling of hermetic seals. The temperature of the joint never rose more than $1^{o}C$ above ambient at any time during reactor operation.

The reaction tube was constructed with a 10mm OD quartz input line leading into the 25mm ID spectrosil reaction tube. The input tube was severely constricted at the point where it entered the reaction tube in order to increase the linear flow rate of the gas and prevent the clogging of the input line with phosphorous. The 25mm spectrosil tube comprised the reaction vessel in which the deposition occurred. Several inches downstream of the point where the seed crystal was placed, a 40mm ID vitrosil tube was attached which extended well beyond the end of the furnace and terminated the reaction tube with a 50/50 male taper joint. The reactor was sealed for normal operation with an endcap fabricated from a 50/50 female taper joint and fitted with a 6mm OD pyrex exhaust line. The purpose of the 40mm tube was to provide a reservoir for the collection of indium chlorides and phosphorus away from the seed crystal while still providing a large enough reaction space so the exhaust line would not clog. The

40mm tube also afforded easy access for the removal of the indium chlorides while eliminating the need for any operations which may have contaminated the spectrosil part of the reaction vessel. The design of Reactor D is illustrated in Figure 1.

The indium source was contained in a spectrosil boat. Two boat designs were utilized, the first (Figure 2a) being simply a 20mm quartz ampoule cut longitudinally along its axis and the second design (Figure 2b) being a section of 20mm quartz tubing cut so that it may accomodate the indium ingot and fitted with a 24mm diameter circular disk with a slot cut into it just at the top level of the ingot at either end. The purpose of the second, more elaborate design was to reduce the size of any stagnant layer or more generally any boundary layer present. By shutting off the gas flow around the boat and forcing the flow to go through the small aperture (the slot in the boat's endpiece), it was hoped that turbulence above the indium melt would increase.

The seed holder was constructed of flat spectrosil plate 20mm on a side supported at a 30° angle relative to the axis of the reactor by a 6mm quartz rod (Figure 2C). The seed holder was designed to rest inside the reaction vessel (25mm bore spectrosil tube) thermally isolated in that area of the vessel with no other quartz ware to p ovide ~ / heat conduction from the seed.

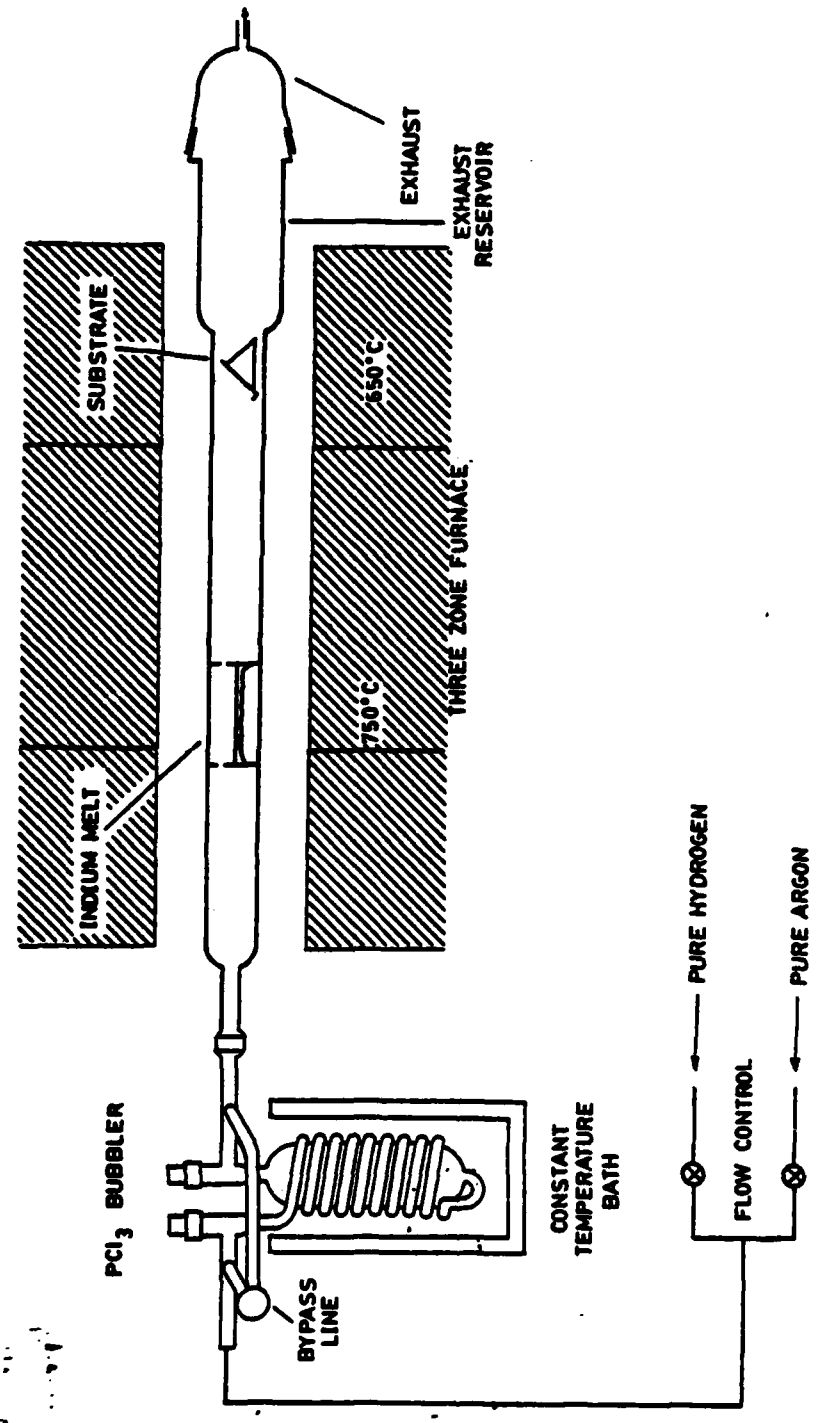

Figure 1 Reactor D.

(a) indium boat (first design)

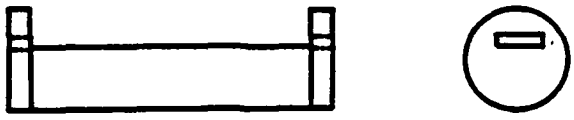

(b) indium boat (second design)

(c) seed holder

Figure 2 Quartz ware for reactor D.

Insertion and manipulation of both the indium boat and the seed holder inside the reactor was performed with a quartz transfer tube to insure minimum contamination of the quartz ware from the waste products which accumulate in the 40mm bore quartz tube.

A Lindberg three zone furnace was used to facilitate control of the temperature profile as well as to provide the means for very quickly cooling the reaction tube. The reaction tube was situated and supported in the furnace with asbestos windings which also served as thermal insulation and as a barrier to convection currents.

3.2 GROWTH PARAMETER CONTROL

In Reactor D, as in other chloride systems, control over the processes governing crystal growth and impurity incorporation was obtained through the control of certain physical parameters. These parameters are flow rate, PCl_3 temperature, indium source temperature, temperature gradient across the In source, substrate temperature, and temperature gradient at the substrate [3].

Control of the reactor's temperature profile was accomplished by adjusting the left and center zones of the furnace in tandom. In order to increase reproducibility and decrease thermal convection currents in the indium melt, the left and center zones were set to provide a four inch length region where the temperature varied by no more than $0.1^{o}C$. The indium boat was situated in this temperature

plateau region. Control of the substrate temperature was obtained by adjusting the right zone of the furnace with the control point being at the center of the seed crystal. The gradient of the temperature at the seed was controlled by moving the seed either closer to the furnace wall for a greater temperature gradient or closer to the center zone for a smaller temperature gradient.

The flow rate of the H_2 was controlled with a pneumatic flow controller and monitored with a rotameter specifically calibrated for H_2. Switching the flow through the bubbler on and off was controlled by the PCl_3 containment valves and the bypass valve.

With the design of the bubbler used and no dilution line, manipulation of the PCl_3 temperature is tandamount to direct control of the input mole fraction of PCl_3. Control of PCl_3 was maintained with the use of a constant temperature bath. The bubbler assembly was placed inside a dewar leaving only the valves and the input/output lines above the level of the pure ethanol used for heat exchange between the bubbler and copper heat exchange coil through which flowed ethanol refrigerated and kept at a constant temperature by a Lauda K2/R circulator. The circulator was capable of achieving stable temperatures as low as $-15.0^{\circ}C$. Special care was taken in designing the bubbler to achieve thermal equilibrium between the H_2 input gas, the PCl_3, and the constant temperature bath in order to

insure complete saturation of the H_2 with PCl_3 at the desired temperature. With this in mind, we are able to compute the input mole fraction of PCl_3 as a function of temperature using equilibrium calculations in the formula:

$$\text{mole fraction } PCl_3 = \frac{\text{moles } PCl_3}{\text{moles } PCl_3 + \text{moles of } H_2} = \frac{P_p V}{P_p V + P_n V} \quad (4)$$

where

P_p = equilibrium partial pressure of PCl_3 (Torr)

P_H = pressure of H_2 (Torr)

V = flow rate cm^3/min.

and finally:

$$\text{mole fraction} = \frac{P_p}{P_p + P_H} \text{ atomic fraction.} \quad (5)$$

The partial pressure of PCl_3 as a function of temperature was graphically obtained from Figure 3 [8] and using Equation 5, the entries of Table 1 were calculated.

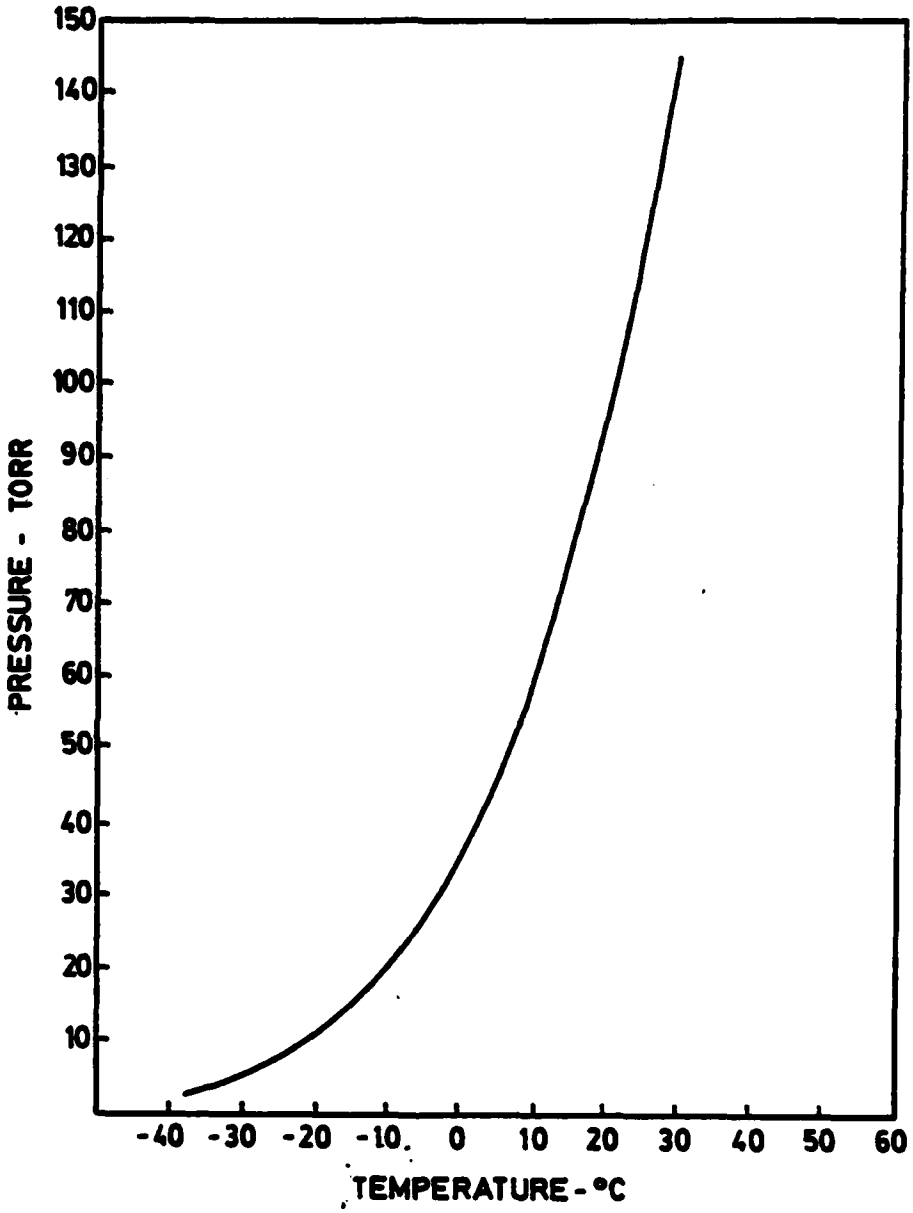

Figure 3 PCl_3 vapor pressure data.

Table 1 - Mole Fraction - Calculated

% Mole %	(^{o}C) Temp PCl_3	(Torr) VP PCl_3
2.0	- 16.0	15.2
2.2	- 14.5	16.7
2.4	- 12.3	18.2
2.6	- 10.8	19.8
2.8	- 8.6	21.3
3.0	- 7.3	22.8
3.2	- 6.8	24.3
3.4	- 6.0	25.8
3.6	- 5.0	27.4
3.8	- 4.0	28.9
4.0	- 3.0	30.4

4. REACTOR OPERATION

4.1 SOURCE MATERIALS

The literature reports that the purity of grown layers is intimately associated with the purity of the starting materials, especially indium [1,6]. The indium used was obtained from Johnson Matthey Chemicals Limited and was AlA grade designated for vapor phase epitaxial work. Each ingot was 50g. The PCl_3 was obtained in both 50g and 100g ampoules from M.C.P. Electronics Limited. Growth runs were performed on iron doped, semi-insulating substrates obtained from Metal Specialties. Three substrate orientations were used: {100}, {211}, and {111}.

4.2 REACTOR MAINTENANCE

The initial set up of the reactor consisted of degreasing in chromic acid and sulfuric acid, then cleaning the reaction tube and the bubbler assembly in aqua-regia for several hours followed with an 18 megaohm deionized (DI) water rinse. Both components were then dried in an N_2 flow and set into position in the furnace. The reaction tube was then baked out for several hours at 850°C.

Loading the PCl_3 into the bubbler was accomplished through the output PCl_3 containment valve. The ampoule was thoroughly cleaned and placed into the transfer container which was then sealed in place over the containment valve and flushed (along with the rest of the reactor) in a high argon flow. An argon overpressure

was then established in the bubbler and transfer container to insure minimum contamination from atmospheric gases. The ampoule was then broken and the contents poured into the bubbler. The containment valve was then replaced and the transfer container removed. Immediately after the supply of PCl_3 was replenished, H_2 flow was reestablished and the reactor was heated to growth temperature. H_2 was then bubbled through the PCl_3 and introduced into the reaction tube to remove the more volatile contaminants from the PCl_3 associated with atmospheric contamination and to further clean the reaction tube.

The boat and seed holder were prepared by degreasing in boiling trichloroethylene (TCE), acetone, and methanol followed with a DI water rinse, then further cleaned for several hours in aqua regia (3:1 $HCl:HNO_3$), rinsed in DI water, and dried in an N_2 flow. Both boat and seed holder were then inserted into the reaction tube using a clean transfer tube. The reactor was sealed and flushed for several hours in H_2, then baked out at the growth temperature and further cleaned by injecting PCl_3 into the reaction tube.

Following the cleaning in the PCl_3 flow, the reactor was flushed with argon and opened. A high flow of argon was maintained when the reactor was opened to inhibit the back-flow of atmospheric gases into the reaction tube. Excessive phosphorus deposition was removed from the wall

of the exhaust reservoir and the boat and seed holder were removed so the indium melt may be installed or a seed crystal put into place.

Reactor maintenance during a series of growth runs consisted of flushing the reactor with argon prior to violating reactor seals, removing the indium chloride and phosphorus deposition from the wall of the exhaust reservoir, removing the grown sample and replacing it with a new seed crystal using the transfer tube, and finally sealing the reactor again. Subsequent to any maintenance performed, the reactor was flushed for no less than two hours with H_2 at a high flow rate before any further steps were taken. This allowed sufficient time for the purging of the atmospheric gas which entered the system as a result of the maintenance.

4.3 GROWTH PROCEDURES

4.3.1 Sample Preparation

The {100} samples were prepared by degreasing in successive baths of boiling TCE, acetone, and methanol, then the work damage was removed through mechanical polishing using a 1% bromine methanol solution. The work damage was normally removed from several large wafers at a time using this method and stored for future use. Prior to insertion of a sample into the reactor, another pre-insertion etch was performed to give a clean surface on which to grow.

The sample was placed in a quartz beaker and once again degreased using the TCE, acetone, and methanol regimen. The sample and beaker were then liberally flushed with clean methanol and the 2% bromine-methanol solution was then added immediately. The etch was performed for four minutes with mild agitation, then terminated with a methanol rinse. The sample was kept under methanol until it was actually inserted into the reaction tube. The degreasing step prior to the pre-insertion etch proved to be necessary to avoid clouding of the sample's surface. Degreasing and keeping the sample under methanol during intermediate steps eliminated the surface clouding without resorting to the KOH rinse reported in the literature [1,9]. Using the above method, smooth layers were obtained easily; however, the substrates contained a large number of stacking faults which made it impossible to achieve a surface free of pits.

To date, there is no satisfactory etch for {111} or {211} material. For these orientations, a slight modification of the procedure used for {100} samples was used. The severe pitting problem occurring with {211}A and {111}A faces necessitated abandoning the mechanical polishing step. The pre-insertion cleaning and etch performed varied from procedure used for the {100} material only in that almost no agitation was applied during the etch. Using this procedure resulted in the removal of much work damage for

{211}A and {111}A faces but the efficacy of the etch was greatly diminished by the severe pitting. Results of the etch on the {211}B and {111}B faces were much better than those obtained for the A faces. Some surface roughness remained after the etch and there was some pitting but this later proved to have very little effect on the morphology of the grown epitaxial layer. Figures 4 thorugh 6 show photomicrographic results of the etch procedures outlined above. A nomarske interferometer was used so surface features are accentuated.

4.3.2 Thermal Cycling

Reiterating a statement made in the section on growth parameters: it is essential to reliably produce a stable reactor temperature profile to maintain control over the growth process. It is also desirable to reduce the total warm-up (as well as cool-down) time since the phosphorus in the system has an extremely high vapor pressure and loss of phosphorus can cause damage to the surface of the substrate and excessive depletion of phosphorus from the indium source. For these reasons, the proportioning on the furnace controllers was set to give a slight overshoot for a given temperature setting. The reactor was allowed to cool to the proper temperature and the controllers were adjusted manually throughout the remainder of the growth run or saturation run so the temperature profile of the entire reactor varied no more than $0.5^{o}C$ at any point within the furnace.

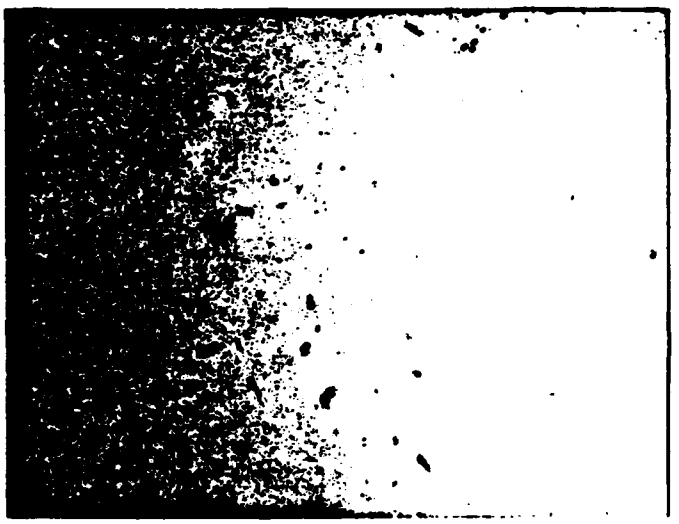

Figure 4 Results of etch on {100} samples.

(a) {111}A surface (110x)

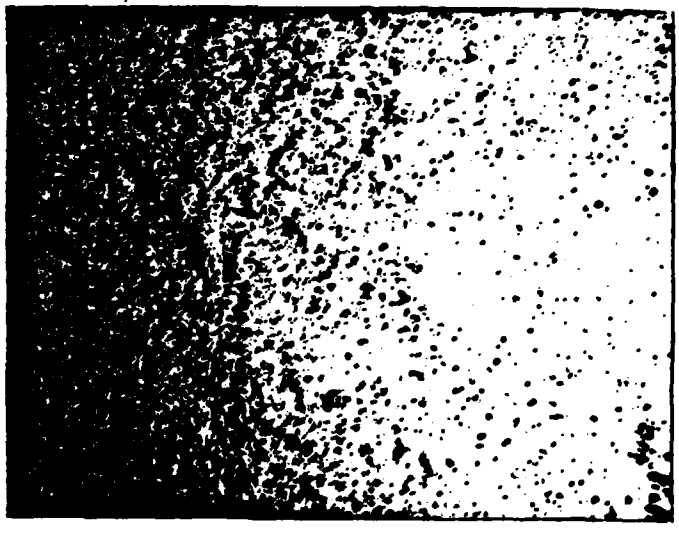

(b) {111}B surface (110x)

Figure 5 Results of etch on {111} samples.

(a) {211}A surface (110x)

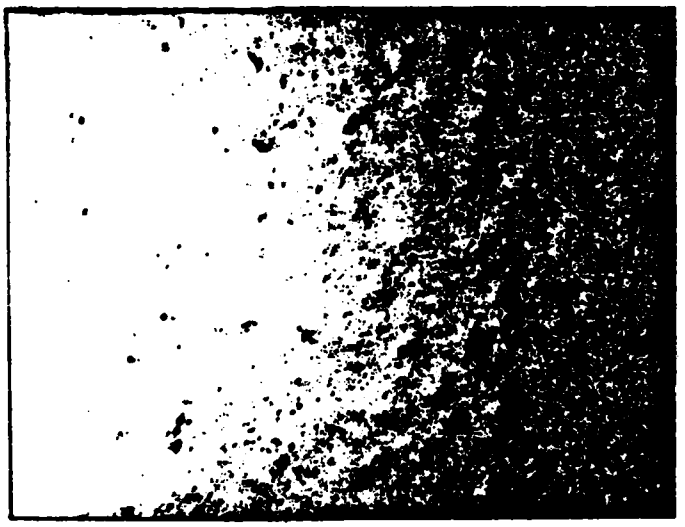

(b) {211}B surface (110x)

Figure 6 Results of etch on {211} samples.

The left and center zones of the reactor were adjusted to provide the very flat temperature profile over the length of the indium boat. The right zone was adjusted to give the proper seed temperature with a temperature gradient at the seed of about 15°C/inch. In the course of the experiments performed, the source temperatures used were 700°C and 750°C. The seed temperature was kept 100°C cooler than the melt temperature with the exception of runs performed to determine the effect of seed temperature on growth. Reactor profiles for the source temperatures used are shown in Figure 7.

4.3.3 Melt Saturation

Subsequent to the insertion of a new indium ingot, the melt must be saturated with phosphorus. For saturation, the reactor was heated to the temperature profile at which later growth runs were to be performed. A PCl_3 flow was then introducee over the indium melt until a thick, InP crust was formed over the indium. The minimum time necessary for the saturation of the melt was based on a phosphorus flux calculation, assuming that during saturation the phosphorus transported was incorporated into the melt. The minimum time for saturation of the melt is expressed by

$$\text{Time for saturation} = \frac{RT_p S(T_m)_x}{P(T_p)f} \text{ moles of indium present} \quad \text{(min.)} \qquad (6)$$

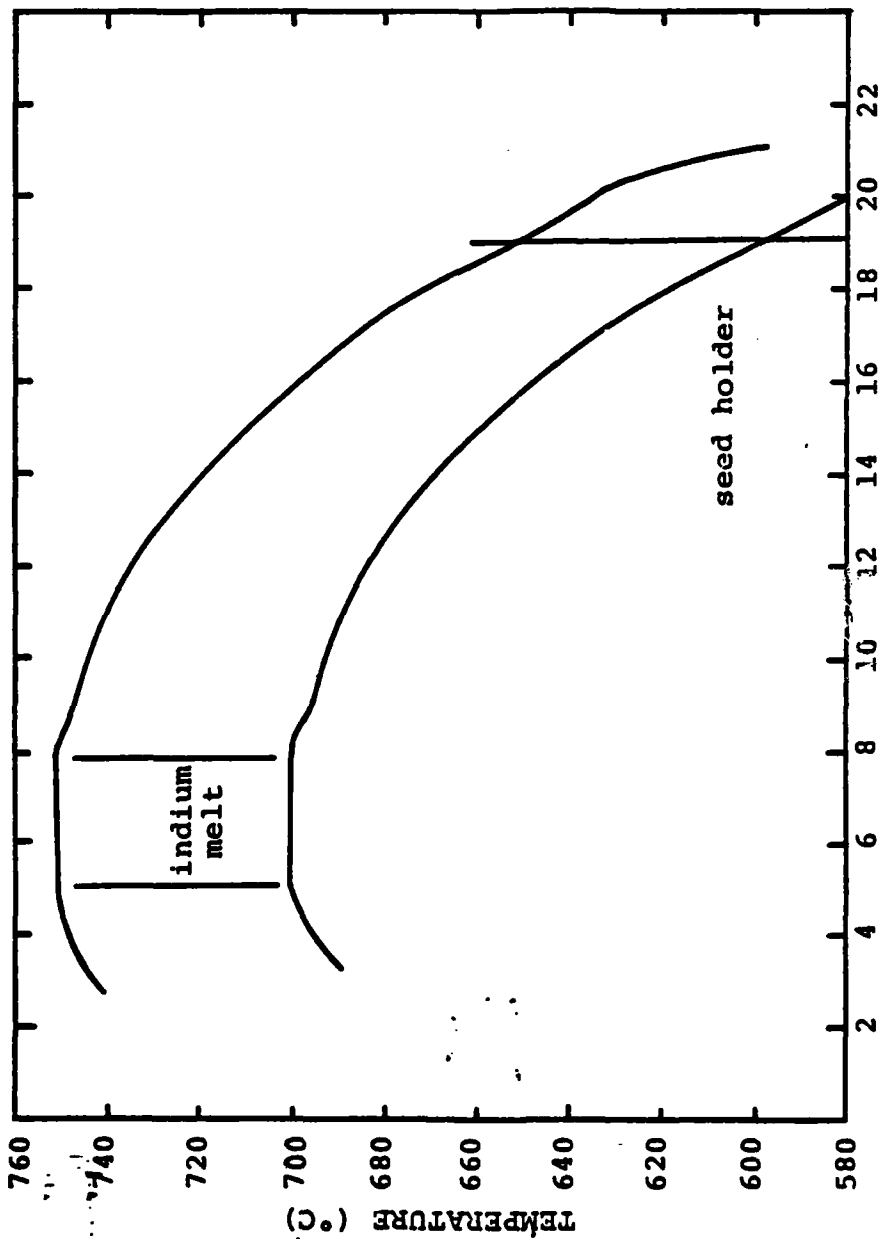

Figure 7 Temperature profile for reactor D.

where

R = ideal gas constant ($\frac{\text{Torr-cm}^3}{\text{Mole-K}}$)

T_p = temperature of PCl_3 (K)

$P(T_p)$ = equilibrium vapor pressure of PCl_3 (Torr)

f = flow rate ml/min.

$S(T_m)$ = solubility of InP in In (atomic fraction) at melt temperature T_m(K)

$P(T_p)$ is obtained from Figure 3 and $S(T_m)$ is obtained from Figure 8 [10].

Actual saturation was typically performed for periods not less than twice the minimum time for saturation to insure full saturation in spite of kinetic factors which may divert some of the phosphorus flux away from the melt.

Extensive melt bake out experiments were performed in an effort to remove high vapor pressure contaminants from the ingot prior to saturation. All bake outs were performed in the presence of a high H_2 flow for periods of from two hours to two weeks at temperatures ranging from 700°C to 850°C. The bake outs ultimately proved to have no effect on growth or purity for growth runs performed at the 750°C source temperature profile.

4.3.4 Growth Procedure

Following the insertion of the seed crystal into the reactor, the entire system was flushed for no less than two hours with H_2 at 150 cm^3/min. and the reaction tube

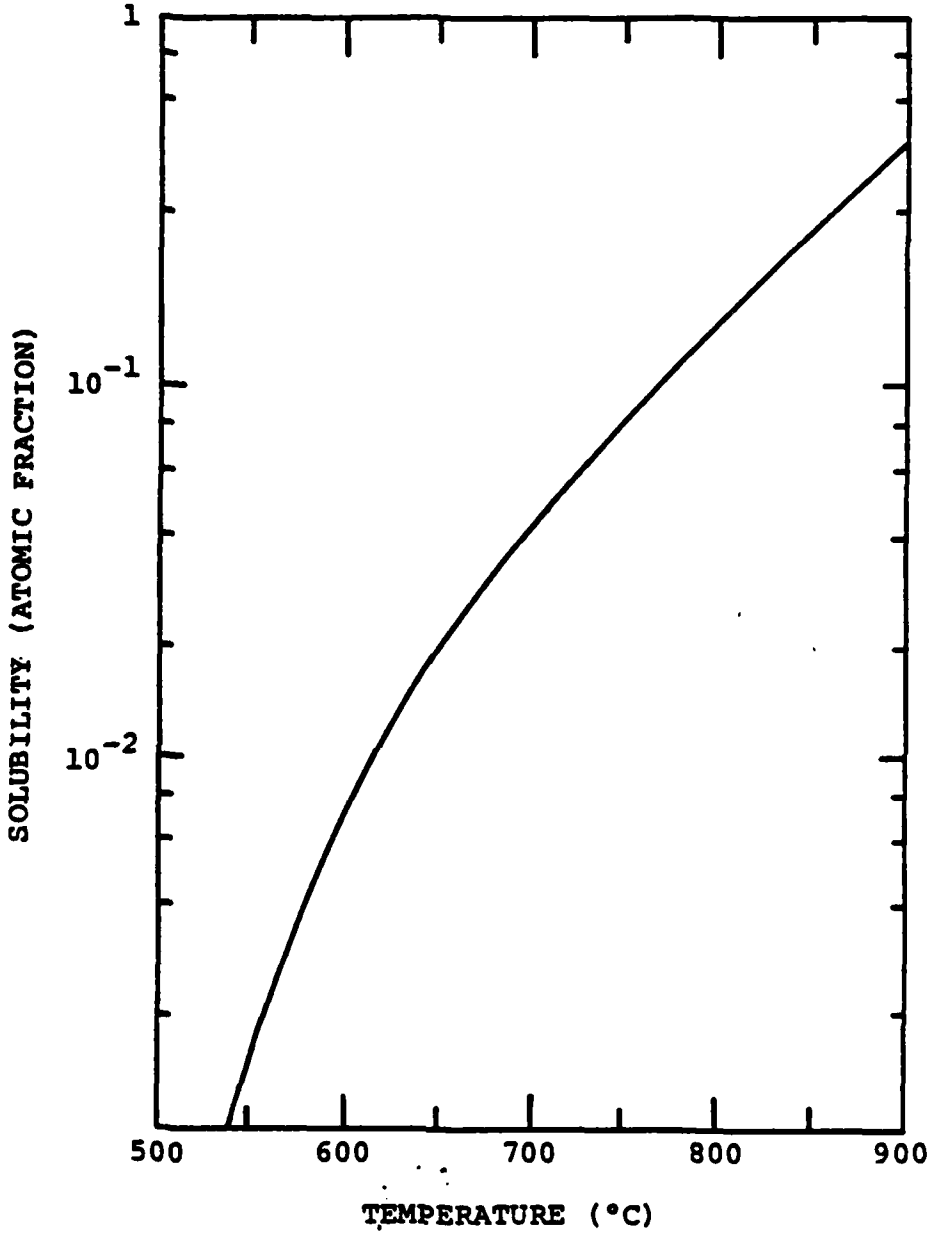

Figure 8 Solubility of InP in indium.

was heated to the growth temperature profile. Prior to growth, it is desirable to remove the surface of the sample (damaged during the reactor's warm-up cycle) while replenishing the phosphorus lost from the surface of the melt. It was found that a satisfactory *in situ* etch of the seed crystal could be obtained simply by maintaining the growth temperature profile during the resaturation of the melt. The paucity of phosphorus in the melt depleted phosphorus from the gas flow downstream of the melt and changed the gas phase stoichiometry at the seed which favored the reaction responsible for etching the surface of the substrate. Measurements made on runs terminated after the *in situ* etch indicated that for {100} substrates, approximately 5μ were removed. The effectiveness of etch was quite striking for {100}, {211}B, and {211}B samples. Nearly mirror smooth surfaces were obtained with almost total disappearance of all work damage accompanied by a reduction in the number of pits seen in the seed crystal. The effect of the *in situ* etch on the {211}A and the {111}A samples was somewhat less effacatious than the results achieved for the other orientations used. The depths of the pits were reduced; however, the remaining pits were still a problem and added to the general surface roughness of the samples.

The growth of the layer commenced when the melt was once again saturated with phosphorus and P_4 transport down the reaction tube could support phosphorus

incorporation into the growing layer. Growth continued with the further input of PCl_3 into the reaction tube. Throughout the entire growth cycle, special care was taken to insure no variation in the temperature profile and that the flow rate remained constant. The growth run was terminated with the opening of the bubbler's bypass valve and the closing of the PCl_3 containment valves followed immediately by shutting off furnace power and opening the furnace to facilitate cooling. The rapid cool down of the reactor was to minimize surface damage to the sample through loss of phosphorus.

During the growth runs, there would appear in the vicinity of the seed crystal and slightly upstream of the seed polycrystalline InP growing on the reaction tube wall. Nucleation and growth of the parisitic polycrystalline material began with the saturation of the melt and continued throughout all growth runs performed. The polycrystalline material which grew during runs on a specific melt was removed as a consequence of the physical replacement of an exhausted indium source with a new ingot. Complete removal of the polycrystalline growth was made easy by the poor adhesion between InP and quartz. Any polycrystalline material not physically removed during melt replacement was etched away during the saturation of the new melt.

Some growth runs were performed allowing the polycrystalline growth to accumulate and some runs were performed in which the polycrystalline growth was removed prior to each new run. Results showed that the presence of the polycrystalline InP had no significant effect on either growth rate or purity.

5. EPITAXIAL LAYER EVALUATION

5.1 SURFACE AND INTERFACE CHARACTERIZATION

5.1.1 Techniques

Evaluation of the physical characteristics of the grown layers routinely consisted of analysis of surface morphology, measurement of layer thickness, and characterizing salient features of the delineated interface (interfacial irregularities, signs of poor surface preparation, crystal strain propagation through the interface, etc.).

The samples were taken as grown and subjected to microscopic examination of the surface of the epitaxial layer. The back surface of the sample was then lapped to a matte finish with 5 μm grit to remove the epitaxial growth from the back of the sample and to facilitate cleaving the sample. Small laminae of the sample were cleaved and the interfaces of each laminae made visible with the use of a delineation etch. The delineation etch [1,9] consisted of immersion of the cleaved sections of the sample for three minutes in a solution which consisted of freshly mixed, equal volumes at room temperature of A and B where

$$\begin{aligned} &\text{(a)} \quad A = 60\text{g KOH} + 250\text{ ml } H_2O \\ &\text{(b)} \quad B = 40\text{g } K_3Fe(CN)_6 + 250\text{ ml } H_2O. \end{aligned} \tag{7}$$

The cleaved sections were rinsed in 18 megaohm DI water

and dried in a N_2 flow. Measurement of the epitaxial layer's thickness was then determined optically while simultaneously determining interfacial characteristics.

5.1.2 Results

Experiments to determine the dependence of growth rates on flow rate, reactor profiles and PCl_3 mole fraction were performed with the source temperature at 750°C. The H_2 flow rate was varied from 60 ml/min. to 150 ml/min. The temperature of the seed was varied from 625°C to 660°C. The range of mole fraction used was from 2% to 4%. Results from the growth runs indicated that growth rate changed for only the orientation of the seed crystal used with the constant 750°C source temperature and was insensitive to changes in the other growth parameters. Figure 9 presents a summary of growth rates for the 750°C indium source for all of the orientations used as a function of the number of growth runs performed on the melt. Figure 9 demonstrates the dependence of growth rate on the melt depletion. The growth rate drops off as the indium melt becomes exhausted.

Growth runs performed with the 700°C source temperature profile and a 150 ml/min. flow rate demonstrated the same growth rate dependence on the number of growth runs performed on the melt while showing the same indpendence on PCl_3 mole fraction as runs performed

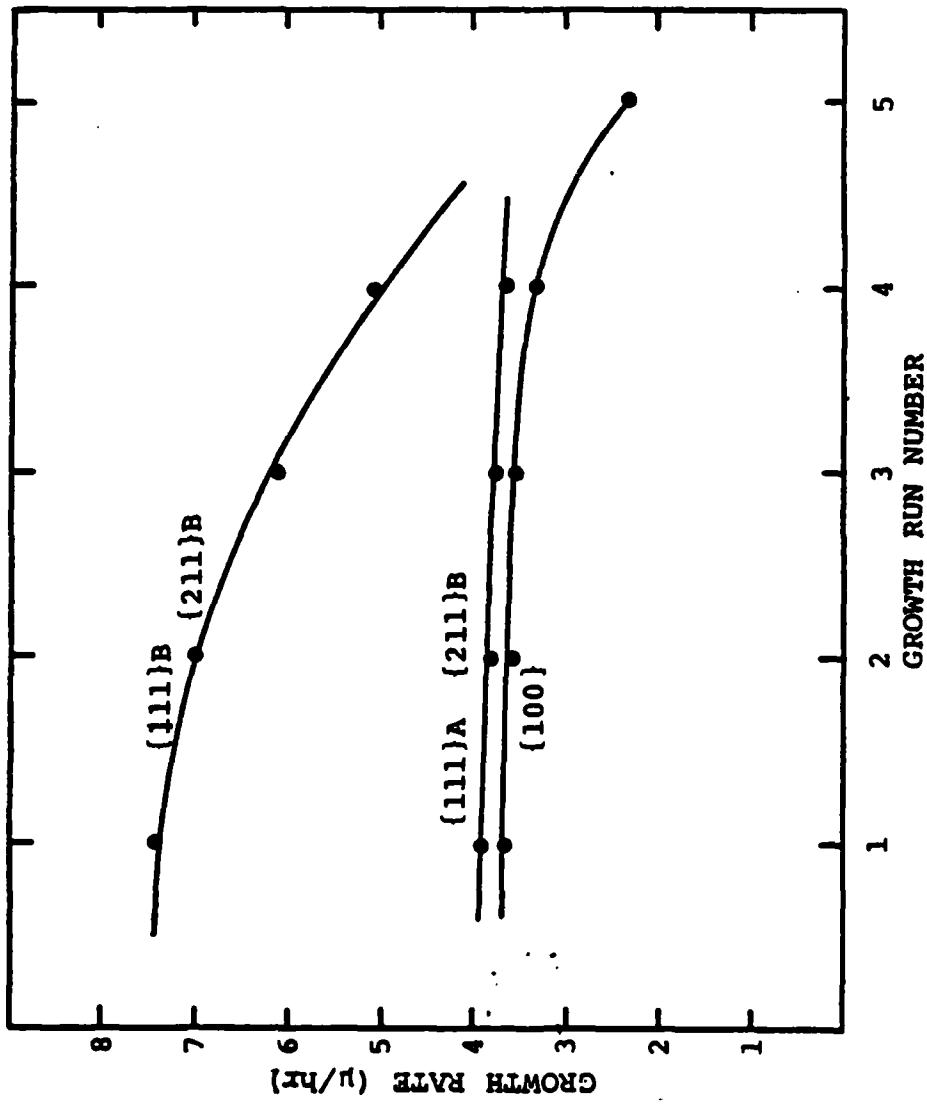

Figure 9 Growth rate summary for samples grown with a 750°C source temperature

at a higher temperature. The growth rate summary for the crystal orientations used is presented in Figure 10.

The insensitivity of the growth rate on flow rate and PCl_3 mole fraction is indicative of saturated growth [6]. In the saturated growth regime, the growth process is dominated by the energetics and kinetics of the reactions occurring at the seed and independent of flux of reactants down the reaction tube. Results show that Reactor D was operating in saturated growth regime for both the 700°C and 750°C source temperature profiles.

For {100} samples grown with the 750°C source profile there was a tendency toward orange peel type surfaces with lower growth rates. Increasing the flow rate to 150 ml/min. yielded surfaces with much less surface roughness though they were not mirror smooth. Lowering the source temperature to 700°C with a corresponding substrate temperature of 600°C and a flow rate of 150 ml/min. gave the best results achieved - mirror smooth surfaces. For all growth conditions used, the epitaxial layer grown on {100} material was homogeneously thick across the entire sample.

The interfaces of samples grown on {100} substrates were generally quite flat and smooth. There would occasionally appear some interfacial irregularity indicative of surface contamination of the substrate. The effect of the surface contamination was to cause roughness

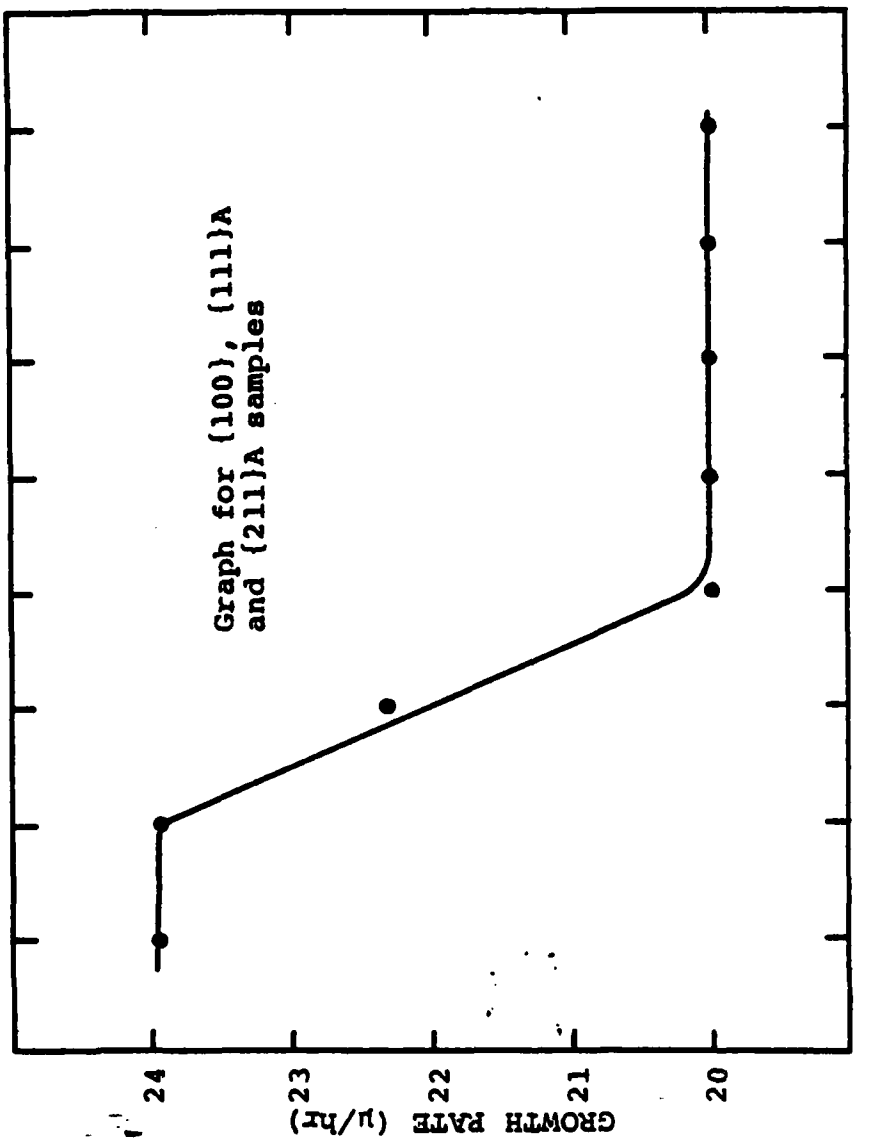

Figure 10 Growth rate summary for samples grown with a 700°C source temperature.

at the interface and strain propagating through the epitaxial layer. Interface roughness also resulted from the stacking faults uncovered in the substrate during sample preparation. The quality of the interface proved to be relatively insensitive to changes in growth parameters.

Typical surface and interface morphologies for samples grown on {100} substrates are shown in Figures 11 and 12 for source temperatures of 750°C and 700°C, respectively.

Growth runs performed on {111}A and {211}A invariably yielded rough, badly pitted surfaces and irregular interfaces. The layers grown were also of inhomogeneous thickness. Using lower reactor temperatures, some improvement in the physical qualities of the surface was obtained in runs performed with the 700°C over the 750°C source temperature profile. Figures 13 through 16 give photomicrographs of typical results obtained from growth runs performed on the indium faces of {111} and {211} with 700°C and 750°C source temperature profiles.

Results of layers grown on the B faces of the {111} and {211} proved to be much better than results from their A face counterparts. The layers grown were homogeneous thick with smooth interfaces for both the 750°C and 700°C source temperature. The surface

(a) surface (110x)

(b) interface (560x)

Figure 11 Typical surface and interface for {100} sample grown with a 750°C source temperature.

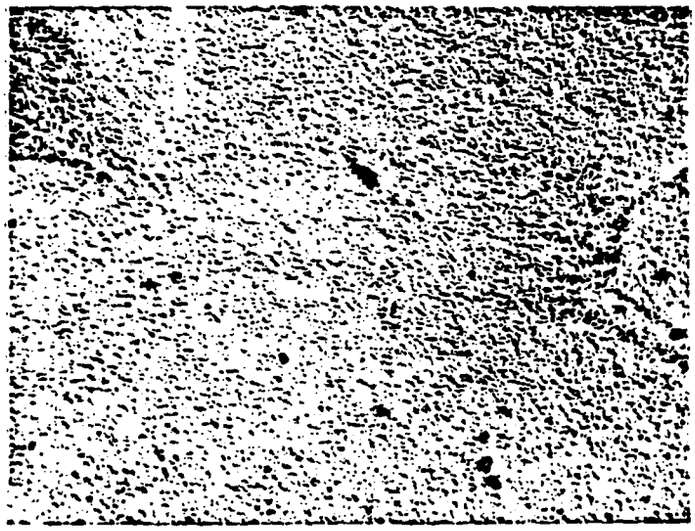

(a) surface (110x)

(b) interface (560x)

Figure 12 Typical surface and interface of {100} samples grown with a 700°C source temperature.

(a) surface (110x)

(b) interface (560x)

Figure 13 Typical surface and interface of {111}A samples grown with a 750°C source temperature.

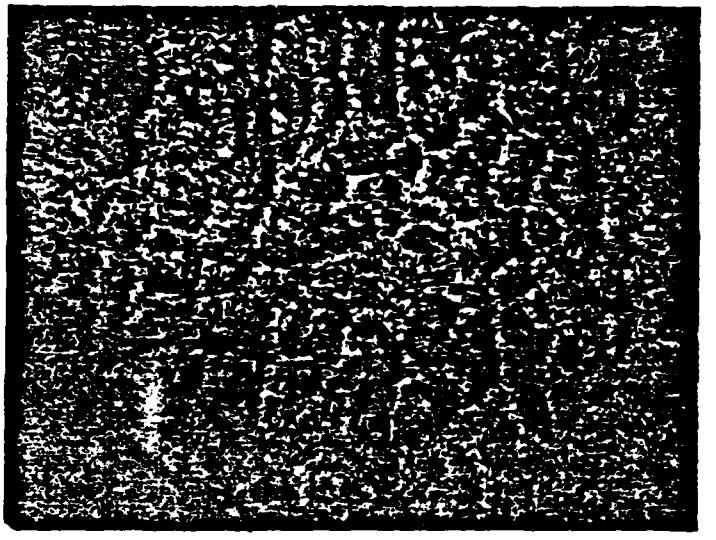

(a) surface (110x)

(b) interface (560x)

Figure 14 Typical surface and interface of {111}A samples grown with a 700°C source temperature.

(a) surface (110x)

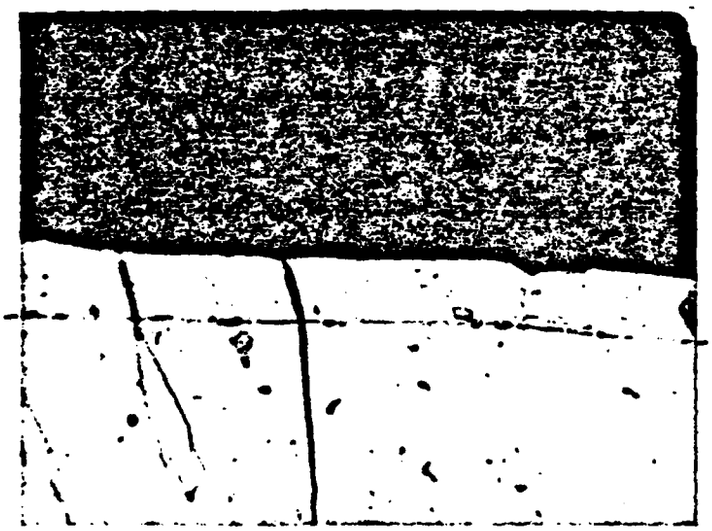

(b) interface (560x)

Figure 15 Typical surface and interface of {211}A samples grown with a 750°C source temperature.

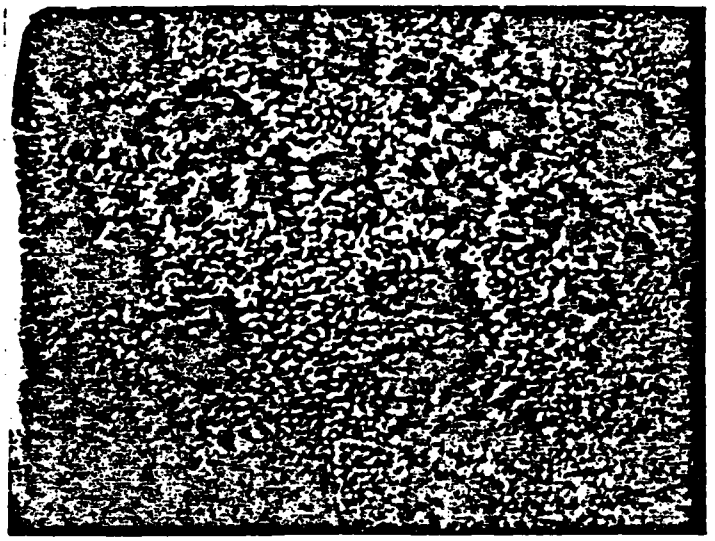

(a) surface (110x)

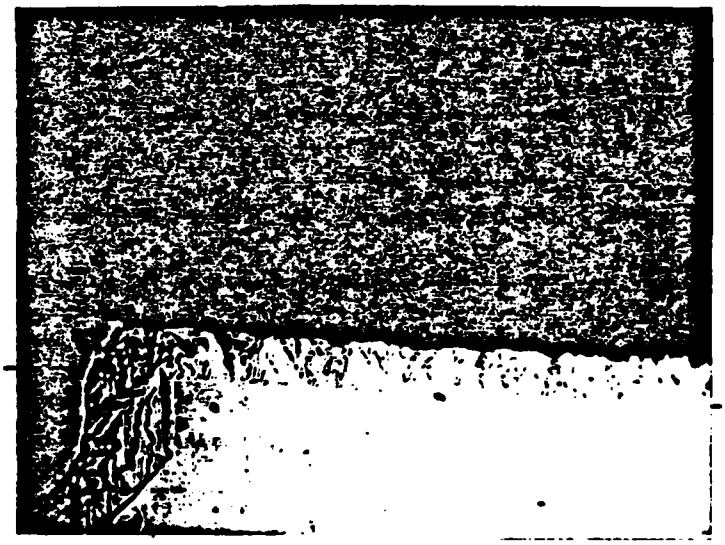

(b) interface (560x)

Figure 16 Typical surface and interface of {211}A samples grown with a 700°C source temperature.

morphology of the samples grown with the lower reactor temperatures was somewhat smoother than those samples grown at higher temperatures; however, the lower temperature growth also brought about the formation of triangular etch pits. The results of growth runs performed on the {111}B and {211}B orientations are shown in Figures 17 through 20. As for the {100} and A faces of the orientation used, the morphology of the layers proved to be independent of flow rate and PCl_3 mole fraction.

5.2 ELECTRICAL CHARACTERIZATION

5.2.1 Techniques

During the microscopic characterization of the grown layers, special attention was given to determine the suitability of the sample for van der Pauw analysis. The sample was checked to confirm that the layer thickness was homogeneous and that there were no pits which extended through the epitaxial layer to the substrate. The failure of a sample to meet these criteria indicates that any data acquired from van der Pauw analysis has a great deal of error and should be held suspect [11,12]. The edges of the sample were then cleaved away to remove the inhomogeneously thick material (which came about due to the gas flow pattern at the edges of the sample during growth) to give a homogeneously thick lamina of regular dimensions. The sample was then placed on a

(a) surface (110x)

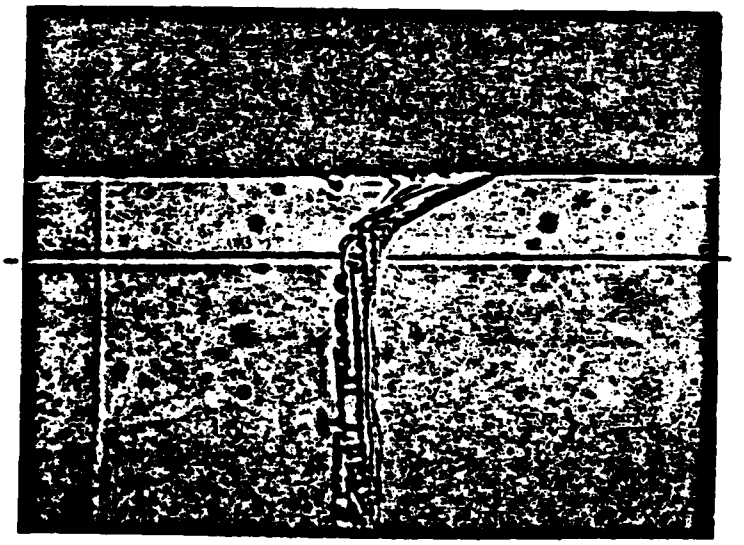

(b) interface (560x)

Figure 17 Typical surface and interface of {111}B samples grown with a 750°C source temperature.

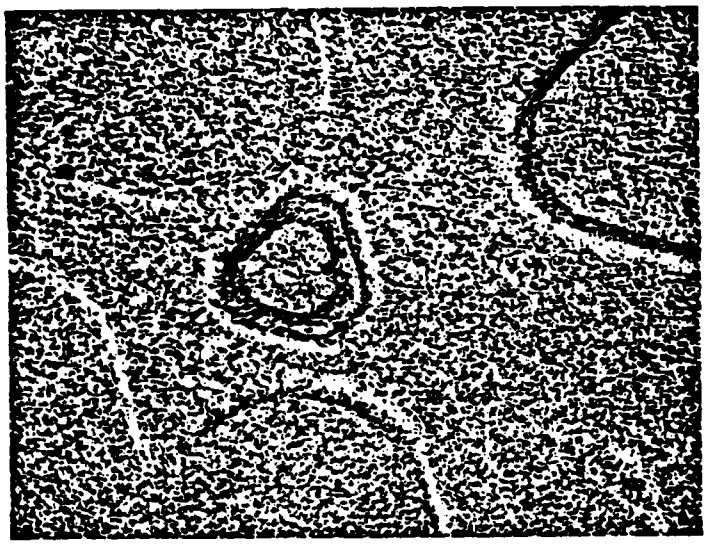

(a) surface (110x)

(b) interface (560x)

Figure 18 Typical surface and interface of {111}B samples grown with a 700°C source temperature.

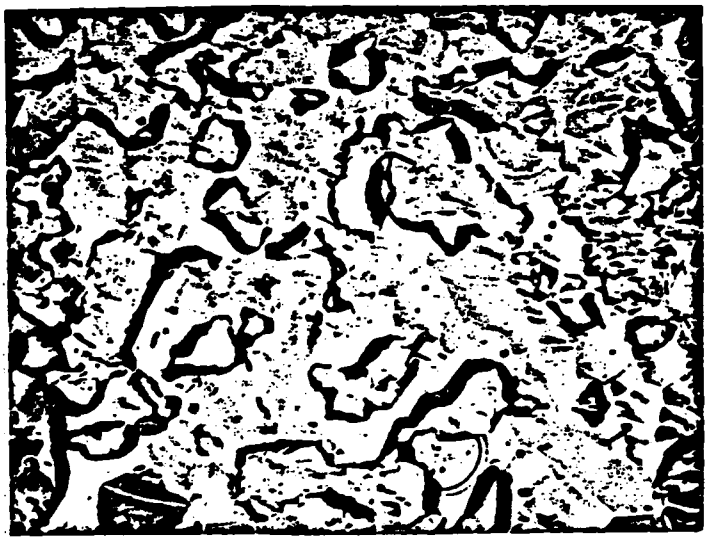

(a) surface (110x)

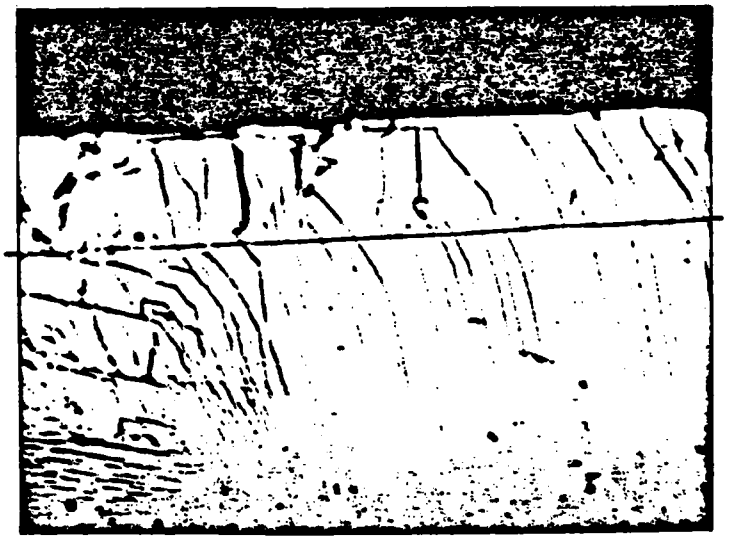

(b) interface (560x)

Figure 19 Typical surface and interface of {211}B samples grown with a 750°C source temperature.

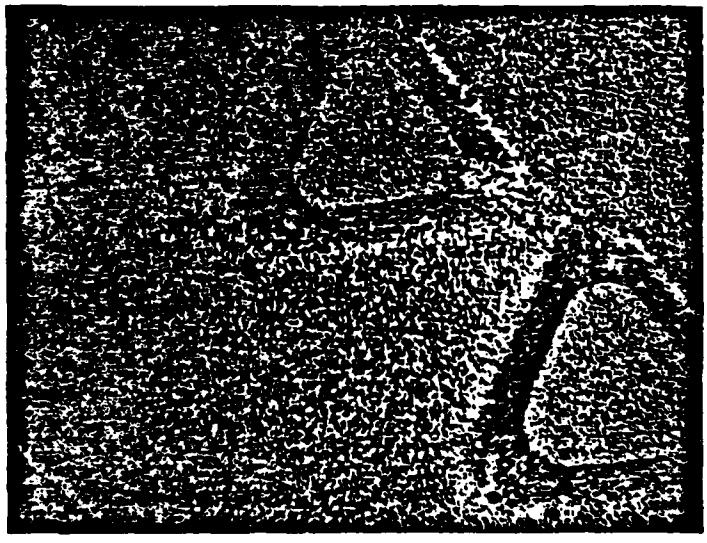

(a) surface (110x)

(b) interface (560x)

Figure 20 Typical surface and interface of {211}B samples grown with a 700°C source temperature.

carbon heating strip and tin spheres were placed at the tip of each corner of the sample. 10 mil tin spheres were used for small samples and 20 mil tin spheres were used for the larger samples. The size and placement of the contacts were chosen to reduce the error made in the measurements [11-14]. The heating strip and sample were then placed in a H_2 environment and allowed to flush for ten minutes. A low flow of HCl was then injected into the system to clean the sample and the spheres to improve the contacts. The sample was heated to 300°C and the tin was alloyed in for approximately two minutes. Power to the heater was then shut off, the HCl flow was terminated, and the system allowed to cool in a H_2 flow. The sample was removed from the alloying station and mounted on a testing block. Electrical contact to the sample was achieved by using thermocompression to attach nickel wire.

The quality of the ohmic contacts was determined by observing the I-V characteristics of the contacts. The I-V characteristics also gave a rough estimate of the sample's resistivity and provided the means of determining the current levels to be used in the measurements to minimize error due to non-linearities in the I-V characteristics [14]. The contacts achieved were normally very good and displayed nearly ideal linearity. Occasionally a sample would lose a contact due to

mechanical stress or thermal stress, and would require re-alloying after the sample was thoroughly cleaned in boiling TCE, acetone, and methanol, respectively. The contact would be re-established using the same alloying procedure outlined above. Contacts displaying non-ohmic characteristics were made to be ohmic through successive heating cycles in a H_2-HCl flow.

The samples were then measured using the method of van der Pauw to determine resistivity and Hall effect. Using this information, the carrier concentration and mobility were then determined using a single band model with the high field limit approximation for scattering mechanisms (measurements were made in a 2.2 kGauss magnetic field) [11-14]. Measurements were typically made at 300K and 77K to determine the presence of any deep donor or signs of compensation evidenced by a large change in the carrier concentration or Hall factor, respectively.

5.2.2 Results

There are several factors which may cause significant error in the van der Pauw measurements, such as a depletion layer at near the substrate epitaxial interface causing a change in effective layer thickness (an effect which would have no effect on measured mobility) and domination of the bulk epitaxial layer properties by a damaged layer at the surface of the sample. We shall

assume that the effect of the interfacial depletion layer is negligible because of the relative insensitivity of the dependence of carrier concentration on layer thickness. The effect of any damage layer in distorting the true reading from samples was evaluated by taking samples grown on the various orientations used, making the van der Pauw measurements, etching down the layer by 5μ, and repeating the measurements. Results indicated no significant change in van der Pauw data as a consequence of the presence of a damage layer as it exists on samples taken directly from the reactor.

Tables 2 through 4 show typical results for samples grown on {111} and {211} substrates with a variety of reactor parameters. The entries indicate that the growth conditions imposed on the reactor by the growth parameters for runs performed on both the indium and phosphorous faces of the {111} and {211} are far from optimum. Since the reactor was being run at near optimum conditions for {100} samples, it is plausible that the poor results obtained for the non-{100} samples are a manifestation of the different thermodynamic properties of the growth kinetics at the surface of the samples for the different orientations. Knowledge of whether the lack of purity is due to impurity incorporation or other stoichiometric defects cannot be accrued using the information presently available. The data presented for the indium faces of

Table 2 - Hall Data For {111}A and {211}A Samples Grown With 750°C Source

Run Number	300K n (cm^{-3})	300K μ (cm^2/V-sec)	77K n (cm^{-3})	77K μ (cm^2/V-sec)	PCl_3 Temp. (°C)
6.3	1.9×10^{15}	793	1.2×10^{15}	3917	- 10.5
8.2	5.6×10^{18}	1200	2.2×10^{18}	4040	- 11.1
8.3	4.4×10^{16}	760	2.3×10^{16}	1530	- 10.0
9.1	6.0×10^{16}	513	2.6×10^{16}	783	- 10.5
9.2	2.5×10^{17}	231	9.2×10^{16}	321	- 10.6
9.3	2.4×10^{17}	141	1.3×10^{17}	1600	- 10.4
11.1	1.6×10^{17}	5424	5.9×10^{15}	22023	- 6.0
11.4	1.7×10^{16}	537	1.1×10^{17}	835	- 6.0
12.2	8.3×10^{16}	1304	1.7×10^{16}	7430	- 7.2
13.4	2.0×10^{17}	583	6.8×10^{16}	1805	- 10.1

(a) {111}A

Run Number	300K n (cm^{-3})	300K μ (cm^2/V-sec)	77K n (cm^{-3})	77K μ (cm^2/V-sec)	PCl_3 Temp. (°C)
6.3	1.5×10^{17}	210	2.3×10^{15}	1889	- 10.5
10.2	2.0×10^{16}	353	5.0×10^{16}	966	- 10.1
11.3	2.6×10^{17}	126	6.9×10^{16}	208	- 6.0
12.1	1.3×10^{16}	1274	1.4×10^{15}	10518	- 6.0
12.3	4.3×10^{16}	1245	1.4×10^{16}	7680	- 11.6
13.1	1.3×10^{17}	1804	6.5×10^{16}	5200	- 7.2

Table 3 - Hall Data For {111}B and {211}B
Samples Grown With 750°C Source

Run Number	300K n (cm^{-3})	300K μ (cm^2/V-sec)	77K n (cm^{-3})	77K μ (cm^2/V-sec)	PCl_3 Temp. (°C)
6.2	1.1×10^{17}	1910	9.8×10^{17}	2820	- 9.5
6.4	3.2×10^{15}	1630	2.4×10^{17}	2010	-10.5
10.4	7.8×10^{17}	250	3.2×10^{17}	1270	-10.1
13.2	2.4×10^{16}	1690	4.7×10^{16}	2070	-10.1

(b) 111 B

Run Number	300K n (cm^{-3})	300K μ (cm^2/V-sec)	77K n (cm^{-3})	77K μ (cm^2/V-sec)	PCl_3 Temp. (°C)
6.1	5.0×10^{16}	510	2.6×10^{16}	780	- 9.5
6.4	2.8×10^{17}	1800	2.7×10^{17}	2200	-10.5
10.3	5.0×10^{17}	500	1.8×10^{17}	530	-10.1
13.4	2.0×10^{17}	580	6.8×10^{16}	1810	-10.1

Table 4 - Hall Data For {111}A and {211}A Samples Grown With 700°C Source

Run Number	300K n (cm^{-3})	300K μ (cm^2/V-sec)	77K n (cm^{-3})	77K μ (cm^2/V-sec)	PCl_3 Temp. (°C)
15.1	8.6×10^{16}	674	2.7×10^{16}	2790	- 9.2
15.3	7.6×10^{16}	202	8.5×10^{16}	320	- 1.2
15.5	2.5×10^{16}	1014	2.8×10^{15}	2980	-10.2
15.7	5.8×10^{14}	986	1.4×10^{14}	9800	-10.2

(a) {111}A

Run Number	300K n (cm^{-3})	300K μ (cm^2/V-sec)	77K n (cm^{-3})	77K μ (cm^2/V-sec)	(°C)
15.2	1.5×10^{16}	270	3.5×10^{15}	2750	- 7.3
15.4	2.3×10^{16}	523	9.0×10^{15}	1960	- 1.2
15.6	3.5×10^{15}	283	2.0×10^{14}	9500	-10.2
15.8	2.5×10^{15}	1630	1.2×10^{15}	1880	- 7.9

(b) {211}A

both the {211} and {111} samples must be held suspect because the layer morphology violates set conditions for making accurate Hall measurements using the method of van der Pauw [11,12].

Results for growth runs performed on {100} substrates with a 750°C source temperature and seed temperature near 650°C are given in Table 5. The results indicate a basic insensitivity to variations in the other growth parameters for a fixed reactor temperature profile. We also note that there is an apparent association with the purity of an entire set of growth runs on a single melt with the purity of the melt. This melt dependence may be attributed to either an impurity innate to each ingot or contamination at the surface of the ingot by storage container, atmospheric gases, etc.

When the source temperature was reduced to 700°C with a corresponding change in seed temperature to 600°C, there was observed a dependence of purity on both PCl_3 mole fraction and the number of growth runs performed on the melt. The results of the 700°C source temperature growth runs performed on $\{1\bar{0}0\}$ substrates are set forth in Table 6; they indicate an apparent clean-up of the system (yielding higher purity) with successive growth runs performed on the melt and a low PCl_3 mole fraction.

Table 5 - Hall Data For {100} Samples Grown With 750°C Source

Run Number	300K n (cm^{-3})	300K μ (cm^2/V-sec)	77K n (cm^{-3})	77K μ (cm^2/V-sec)	PCl_3 Temp. (°C)
1.1	8.5×10^{15}	1440	4.6×10^{15}	16730	- 0.5
1.3	9.8×10^{15}	2370	5.1×10^{15}	14200	- 0.5
2.1	7.7×10^{16}	1620	3.2×10^{16}	5650	- 0.5
2.2	7.0×10^{16}	2000	3.0×10^{16}	9850	- 0.5
2.3	5.8×10^{15}	1670	1.6×10^{15}	21820	- 0.5
3.1	5.5×10^{15}	2220	2.5×10^{15}	10880	- 0.5
3.2	6.0×10^{16}	290	8.3×10^{15}	2900	- 0.5
3.3	6.5×10^{15}	2220	3.0×10^{15}	24580	- 0.5
3.4	9.3×10^{16}	350	1.0×10^{16}	8120	- 0.5
3.5	4.2×10^{16}	1880	2.0×10^{16}	1070	- 0.5
3.6	5.0×10^{16}	990	1.3×10^{16}	8160	- 0.5
4.1	2.7×10^{15}	880	5.2×10^{15}	5460	- 0.5
4.2	2.1×10^{15}	1680	5.9×10^{14}	11000	- 0.5
4.3	1.0×10^{16}	1830	4.0×10^{14}	34000	- 0.0
4.4	1.0×10^{16}	1640	2.3×10^{15}	28490	- 0.0
4.5	4.7×10^{15}	2180	1.6×10^{15}	28820	- 0.0
5.1	2.0×10^{15}	750	4.6×10^{14}	2080	-10.1
5.3	3.0×10^{15}	2710	2.0×10^{15}	34700	-10.0
7.1	3.0×10^{15}	190	3.0×10^{15}	980	-10.0
7.2	1.8×10^{15}	830	4.8×10^{14}	13000	-10.0
8.1	2.4×10^{16}	2370	1.7×10^{16}	6920	-10.0
8.2	6.4×10^{16}	2230	3.5×10^{16}	7250	-13.2
8.3	5.8×10^{16}	2470	3.1×10^{16}	8100	-10.0
8.4	2.0×10^{17}	1740	1.8×10^{17}	2468	-11.0
9.1	7.6×10^{15}	2310	3.5×10^{15}	23800	-10.5
9.2	9.0×10^{15}	2080	4.0×10^{15}	22280	-10.6
9.3	3.3×10^{15}	1930	1.4×10^{15}	17470	-10.4
9.4	8.2×10^{15}	4380	8.2×10^{15}	18000	-10.8
10.1	9.5×10^{15}	2880	4.7×10^{15}	18840	-10.1
10.2	7.0×10^{16}	1100	2.0×10^{16}	8900	-10.1
10.3	3.0×10^{16}	2670	1.7×10^{16}	10570	-10.1
10.4	6.7×10^{16}	2170	3.0×10^{16}	7900	-10.1
11.1	5.6×10^{16}	1180	1.4×10^{16}	13000	- 6.0
11.2	9.0×10^{16}	930	2.0×10^{16}	7720	-15.4
11.4	2.6×10^{17}	2800	6.9×10^{16}	2080	- 8.9
12.1	4.4×10^{16}	1450	2.0×10^{16}	9960	- 6.0
12.2	5.0×10^{16}	1870	2.3×10^{16}	11120	- 7.2
12.3	1.4×10^{17}	1260	5.0×10^{16}	6980	-11.6

Table 6 - Hall Data For {100} Samples
Grown With 700°C Source

Run Number	n (cm^{-3})	μ (cm^2/V-sec)	n (cm^{-3})	μ (cm/V-sec)	PCl_3 Temp. (°C)
15.1	5.7×10^{16}	1600	1.6×10^{16}	11,000	- 9.2
15.2	8.7×10^{15}	1510	2.5×10^{15}	15,000	- 7.3
15.3	1.2×10^{16}	1390	3.7×10^{15}	11,100	- 1.2
15.4	1.3×10^{16}	1440	3.4×10^{15}	10,500	- 1.2
15.5	2.4×10^{15}	2140	7.5×10^{14}	54,600	-10.2
15.6	6.8×10^{15}	1320	9.6×10^{14}	40,810	-10.2
15.7	8.6×10^{14}	3120	4.6×10^{14}	48,260	-10.2
15.8	2.1×10^{15}	4130	2.1×10^{15}	46,216	- 7.9
16.1	1.3×10^{16}	2640	5.3×10^{15}	17,600	-10.2
16.2	5.0×10^{15}	3210	4.0×10^{15}	19,066	-10.2
16.3	3.8×10^{15}	3723	2.6×10^{15}	28,600	-10.2
16.4	6.9×10^{15}	2700	4.3×10^{15}	2,300	-10.2
16.5	5.5×10^{15}	2880	2.8×10^{15}	2,600	-10.2
16.6	4.3×10^{15}	3040	2.1×10^{15}	31,600	-10.2
16.7	3.0×10^{15}	3360	2.3×10^{15}	28,200	-10.2
16.8	5.9×10^{15}	1580	4.2×10^{15}	11,400	-10.2
17.1	1.6×10^{16}	2540	5.0×10^{15}	12,000	- 9.0
17.2	5.0×10^{15}	2800	2.8×10^{15}	20,000	- 7.3
17.3	3.2×10^{15}	2960	1.5×10^{15}	24,000	- 1.0
17.4	3.6×10^{15}	2840	1.7×10^{15}	25,000	- 1.3
17.5	2.8×10^{15}	2480	1.4×10^{15}	37,900	-10.2

There was observed a dependence of purity on the PCl_3 input mole fraction when the 700°C source temperature profile was used. Also associated with growth runs performed with the 700°C source temperature was the apparent purification of the indium source evidenced by the gradual increase in the purity of the samples grown with successive growth runs performed on a melt.

Experiments were performed to determine the effect of varying the PCl_3 mole fraction during the lifetime of a melt. The saturation and first growth run on the melt were performed at a low mole fraction and the mole fraction was increased with each successive growth run. For the final growth runs performed on the melt, the PCl_3 mole fraction was returned to the low mole fraction of the original growth run. With the return of the mole fraction to its original level, there appeared a large increase in the purity of the material over the first run on the melt. This was taken as being further evidence of *in situ* melt purification. The results of growth runs performed with the 700°C source temperature profile are set forth in Table 6.

6. REACTOR MODEL

In order to obtain an understanding (at least a qualitative understanding) of the effects of the growth parameters on the purity of the epitaxial layers, it is necessary to model the processes which control the transport and incorporation of the impurity responsible for the doping of the samples. The model shall be developed within the constraints imposed by the design of a generalized PCl_3-In-H_2 reactor. The processes germane to the discussion of impurity incorporation shall be identified and examined. The interrelationships of these processes and their dependence of the growth parameters shall be determined. Finally, a function will be defined which analytically relates the purity of the sample to the growth parameters.

The ultimate success or failure of a proposed model lies in the model's ability to explain empirical data and to predict results for a given set of conditions which are meaningful within the limitations inherent in the model. In order to determine if the model developed is reasonable and self-consistent, it sahll be employed to explain the results obtained from Reactor D and, by utilizing the information gained, used to determine a set of optimum growth parameters to obtain higher purity.

References made in the development of the model to either specific results from growth runs or general trends all relate to experiments performed on {100} substrates. The results of runs performed on non-{100} substrates indicated that drastic alteration of reactor conditions needed to be made to obtain any improvement over the results achieved. Also, any effect of the change in growth conditions appeared to be masked by the growth features resulting from the inadequate preparation of the {111} and {211} surfaces.

6.1 GENERALIZED REACTOR DESIGN

It shall be assumed that the reaction vessel is composed of an open tube fabricated with quartz which may react with some of the chemical species present in the reactor. A gas stream of known composition and flow rate is introduced into the reaction tube. Upon contact with the reaction tube wall, the gas reacts with the quartz then passes over the indium source which may be completely or partially covered with a solid InP crust with the presence of some boundary layer above the melt. It will be assumed that the physical dimensions and shape of the melt do not change during the course of a growth run to eliminate the time dependent factors associated with a change in the boundary layer reaction kinetics. The gas stream then flows through

a further length of chemically reactive reactor vessel and passes over the InP substrate where it reacts with the surface of the seed through the boundary layer associated with the seed. Products from the reactions leave the reactor through an exhaust line. The temperature profile of the reactor is postulated as being a profile which is capable of supporting growth and as a function of the distance along the length of the reaction tube alone (Figure 21). It is also recognized that the source materials contain some concentration of impurities. During a growth run, it is assumed that the system achieves some steady state.

6.2 IMPURITY INCORPORATION

Now that we have defined the general reactor in which growth is performed, we must determine and discuss the factors which control incorporation of impurities into the epitaxial layer. To maintain generality, no assumption will presently be made identifying either the chemical species or the mechanisms of the reactions occurring at the surface of the sample other than some reaction takes place which incorporates an impurity at a rate controlled by the thermodynamics of the reaction and the environment of the reactor [15,16]. The "environment" of the reactor is the temperature at the seed crystal, the temperature gradient, and the composition of the gas stream at the seed. The thermodynamics

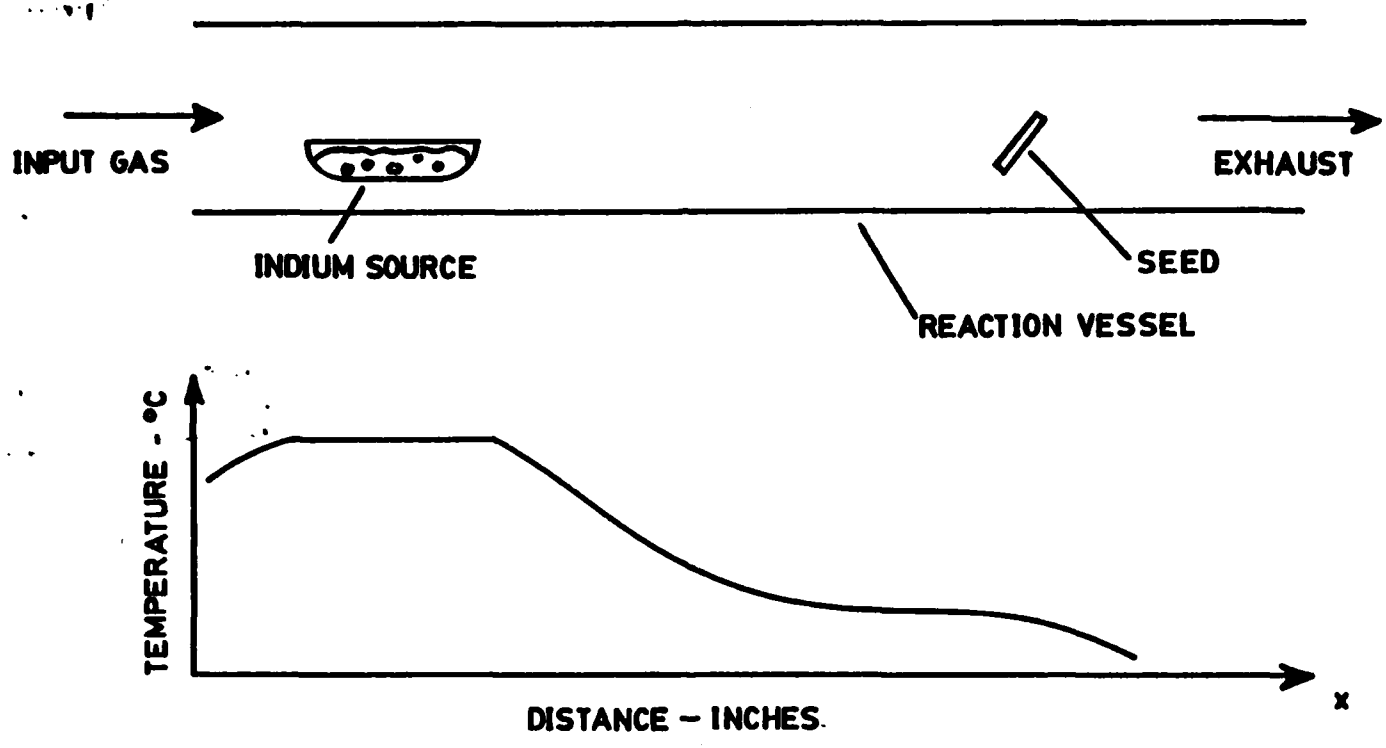

Figure 21 General Reactor Design

refers to the energies of the reaction i.e changes in enthalpy and entropy. Of course, the composition of the gas stream is controlled by processes upstream of the seed which include stoichiometry of the input gas, reaction of the input gas with the reactor, reaction with the indium melt, and reaction of the products of the melt reactions with the reactor. Impurities may be injected into the system in the input gas or as a product of any of the subsequent reactions. Figure 22 shows a flow chart for all the possible reactions which may occur in the reactor. The flow chart shows all reaction schemes because different reactions may occur (or become dominant) for different reactor conditions. Internal to each processing block (and yet unspecified) are the identity of the reacting chemical species and the mechanisms by which the reactions occur.

To simplify the modeling of reactions at the indium melt the assumption shall be made that the InP crust extends across the surface of the melt. By limiting the temperature gradient across the melt, this condition can be easily achieved. The effect of exposed indium during the melt is discussed by Clarke *et al* [3] and may be easily included into the model by taking into account the change in gas stream stoichiometry as a result as well as adding reactions of indium with the gas stream. Assuming that there is an InP crust over the entire melt does not greatly restrict the use of the

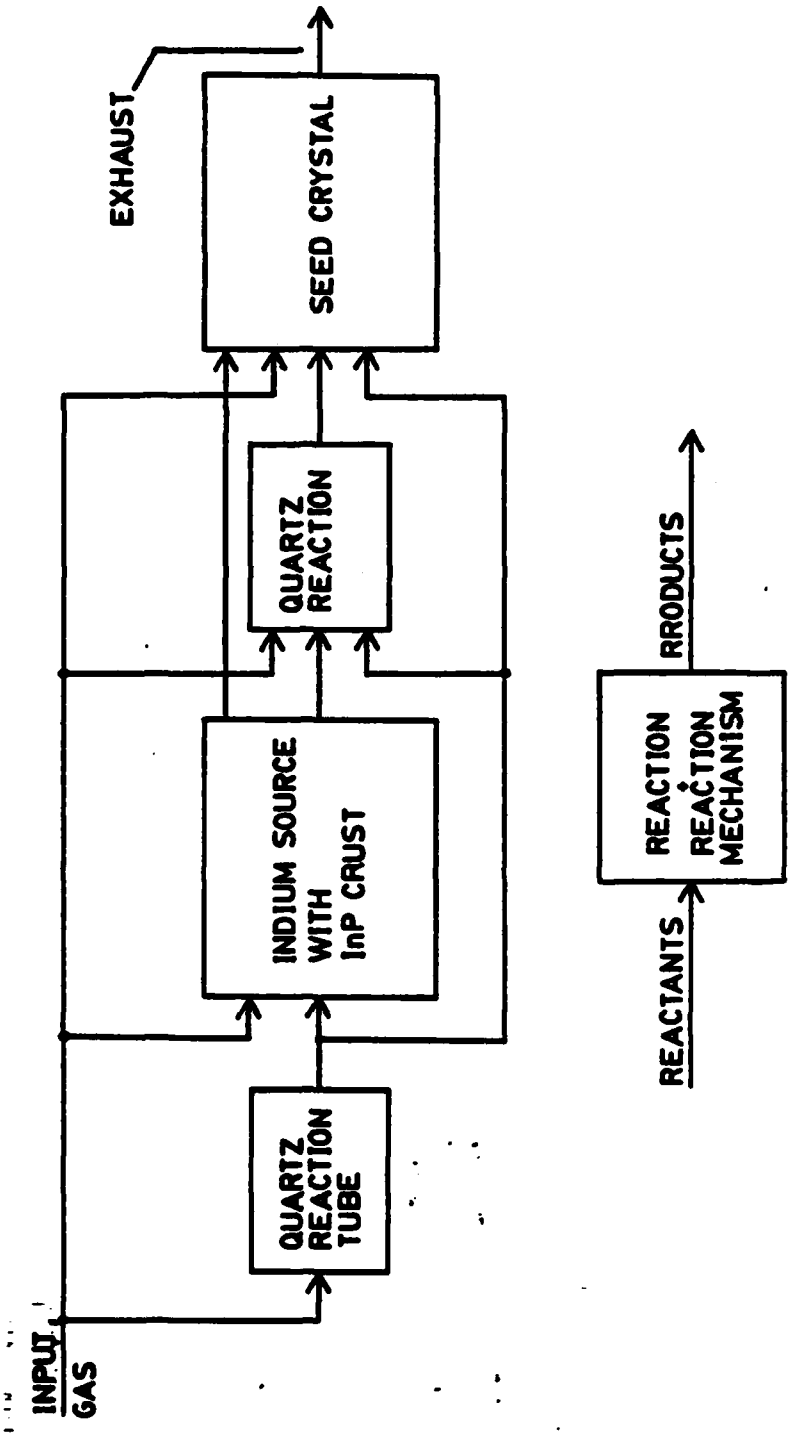

Figure 22 Flowchart of possible reactions.

model since most systems are operated complying to this condition to insure reproducibility. With the above assumption made, the reactions occurring at the melt are controlled by the temperature of the melt and stoichiometry of the gas stream above the melt. The stoichiometry of the gas flow above the melt is dominated by the input mole fraction of PCl_3.

6.3 INCORPORATION FUNCTION DEVELOPMENT

As a consequence of the chloride system design and general factors controlling reactions in the system, it is obvious that changing conditions at some point in the reactor, everything downstream is affected (though not generally in a linear way).

The use of an open tube system with mass transport means that equilibrium is never achieved within the reactor. Recognition that the system is not operated in equilibrium or near equilibrium forces abandoning the use of equilibrium thermodynamics quantitative calculation power while retaining only the ability to predict whether it is energetically favorable for a proposed reaction to occur. Non-equilibrium conditions also force complication of the model with the inclusion of boundary layer at both the indium melt and the seed crystal and mass transport.

Reaction of gas phase chemical species with the solid InP crust of the melt and at the substrate forces

the classification of any over-all reaction mechanism as being heterogeneous and requires using mass transport in modelling the system. Therefore, for the reaction which produces some product i, we must express the reaction rate [17] as:

$$r_i = \frac{1}{V_s}\frac{dN_i}{dt} = \frac{\text{moles of i formed}}{(\text{volume of solid})\ (\text{time})} \tag{8a}$$

or in general

$$r_i = f\ (\text{state of the system}) \tag{8b}$$

where

$$f\ (\text{state of the system}) = ae^{E/kT}g\ (\text{composition}) \tag{8c}$$

a = proportionality constant

E = activation of the reaction

g (composition) = concentration dependence of r_i

where the exponential term of Equation 8c is obtained from the Arrhenius law.

6.3.1 Incorporation Function Statement

Equation 8c tacitly implies knowledge of the mechanism by which the reaction takes place. Thus, to use the model further, we must assume some mechanism or mechanisms which are responsible for the incorporation of the impurity into the layer as well as assume the mechanisms for the growth reactions. Knowledge of the incorporation and growth is necessary because we are

dealing with doping a growing layer where the final concentration (cm^{-3}) is dependent on both impurities incorporated (cm^{-2}-min^{-1}) and growth rate (cm/min) through:

$$\text{Impurity conc.}\,(cm^{-3}) = \left(\frac{\text{Impurity}}{cm^2\text{-min}}\right)(\text{growth rate})\left(\frac{cm}{min}\right)^{-1} \quad (9a)$$

$$\text{and IMPINC} = \frac{\text{Impurity incorporated}}{cm^2 - min} \,. \quad (9b)$$

For such a heterogeneous system with many chemical species and possibilities for reactions present, the possible reaction mechanisms may run the gamut from the simple serial or parallel reactions to complex chain or nonchain reactions with a number of intermediates and molecularity as high as three [17]. Thus, whenever we use the model and its incorporation function, IMPINC it must always be within the context of some set of proposed reaction mechanisms. With some specified mechanism, we may write concisely and generally:

$$\text{IMPINC=IMPINC(FR,MF,CG,CS,TM,DM,EM,DMT,TS,VTS,DS,DST,ES)} \quad (10)$$

where FR = Flow rate

MF = Mole fraction of PCl_3

CG = Concentration of impurity in PCl_3 input

CS = Background concentration of impurity in the reactor

TM = Temperature of the melt

DM = Diffusion Constant of impurity in gas

EM = Activation energy of melt reaction

DMT = Boundary layer thickness at melt

TS = Temperature of substrate

∇TS = Gradient of temperature across the substrate

DS = Diffusion constant of impurity

DST = Boundary layer thickness at the seed

ES = Activation energy of reaction at the seed.

The first seven variables in the argument of IMPINC are the flux variables since they are responsible for the transport of impurities in the system. The last four variables are those variables which directly control the incorporation. Hidden in the above variables is the temperature dependence of the diffusion constants on temperature and the dependence of boundary layer thickness on both temperature and flow rate.

Using Equations (8c) and (10) we may write [17]

IMPINC = exp (TS·EM+TM·ES)/k(TS·TM) g(composition (11)

where g(composition) is some complicated function of the non-energy variables of IMPINC.

One simplification may be employed here. If the proposed mechanism has a step which has a much ~~lower~~ higher activation energy than the other steps, then the ~~low~~ high activation energy step represents the rate determining

step and may be used alone in the model. Otherwise the energy used in Equation (11) is some combination of all the steps in the proposed reaction mechanism.

The compositional dependent part of Equation (11) contains the dependence on the boundary layers, inherent impurity concentration, and flow rate. The form of g(composition) is intimately related to the reaction mechanism and cannot be specified without complete knowledge of the mechanism.

6.3.2 Complications

Ideally, the function IMPINC should provide a single number for the impurity concentration predicted for given growth conditions; however, there are problems associated with trying to obtain a good quantitative result. The correct reaction mechanism or mechanisms must be used in the model and choosing the proper reactions from all the possibilities requires fitting the model to experimental results. More than one proposed mechanism may fit the empirical data but fail to predict the outcome of experiments using a different set of reactor conditions. There may be no unique, overall mechanism [17].

Use of IMPINC for quantitative predictions requires exact knowledge of diffusion "constants" as a function of temperature for each proposed impurity. These constants must be experimentally obtained and determining

them constants for reactions at the melt and seed would be very difficult. Determining the thickness of a boundary layer and its dependence on temperature and flow rate is very difficult because of the dependence on reactor design and the physical shape of the melt (which changes from run to run).

The functional form of IMPINC is very difficult to determine because of the dependence of reactions on other reactions which occurred upstream. Another complicating factor which obscures the form of IMPINC is the inability to change only one of the variables in the argument of IMPINC at a time. The problem of determining the form becomes non-linear and depends on the relationships between IMPINC variables and growth parameters. Figure 23 shows the relationship between those controllable variables of IMPINC and the growth parameters ("x" indicates dependence).

	FLOW RATE	PCl_3 TEMPERATURE	REACTOR TEMPERATURE
FR	X		
MF		X	
TM			X
DM			X
DMT	X	X	X
TS			X
DS			X
DST	X	X	X

Figure 23 Interdependence of IMPINC variables through the growth parameters.

7. IMPURITY INCORPORATION MODEL APPLICATION

With all of the above complications taken into account, the usefulness of the model as a quantitative tool is reduced to almost nothing; however, when the model is used in conjunction with equilibrium thermodynamic data (recognizing that the data is not entirely correct) and experimental data, some general trends may be resolved. These general trends give a qualitative understanding of certain reactor processes and may be used to indicate changes in growth parameters to yield desired results. One word of caution; trends indicated without specific knowledge of the effect of each IMPINC variable containing a design dependence may give different results for reactors of dissimilar design.

It was cited in Section 5.2.1 that no mole fraction effect was observed at the 750°C source temperature profile accompanied by an insensitivity of growth rate on H_2 flow. The only change in purity associated with the 750°C source temperature occurred as a result of changing the melt (indicating a dependence of the purity of the grown layers on some impurity intrinsically present in the indium melt). Reduction of the source temperature to 700°C with a corresponding reduction in the seed temperature to 600°C was accompanied by the observation of reproducible changes in the purity of grown layers with changes in

PCl_3 mole fraction. There was no apparent change in growth rate with changes in mole fraction at the 700°C source temperature profile. Also observed with the 700°C source temperature was a curious increase in purity for samples grown at a given mole fraction of PCl_3 when intermediate runs were performed at a much higher PCl_3 mole fraction.

In this section we shall apply the model developed in this paper to Reactor D in order to determine qualitative identification and explanation of the processes responsible for the results cited above. In order to use the model it shall be necessary to assume mechanisms which lead to self-cosistant results within the model, but the mechanisms proposed need not be the only ones which fit the empirical results.

The model developed in this paper may be applied independently to different impurities being incorporated into the same layer provided there is no interaction between the impurities and that the reactions change the stoichiometry of the entire gas stream very little. These two conditions as stated are very much the same thing; however, the former condition demands the different impurity reactions occur in parallel and the latter condition insures that each reaction may be modeled independently of any other impurity. In modeling the processes occurring in the reactor, we shall postulate the existence

of two impurities being incorporated into the growing layer, one associated with the reactions of the gas stream with the reactor and the other associated with the indium source.

7.1 GENERAL TRENDS

The independence of purity on growth parameters for a 750°C source temperature profile may be explained using the model set forth in this paper in conjunction with a modification of the model proposed by DiLorenzo [3,5] to explain the mole fraction effect in GaAs or by using the IMPINC model with an impurity present in the melt. Both explanations hinge on the assumption that the rate of impurity incorporation being dominated by the energetics of the surface reactions involving the growing layer and the impurity (variations of the other factors affecting incorporation with changes in the growth parameters demand this). However, if the doping of the sample were due solely to the chlorosilane reactions [3], the results would be consistent with every melt used but variable with growth parameters. Experimental results show this is not the case.

Assuming that there is some impurity native to the indium source at some concentration which varies from ingot to ingot, the melt dependence of the result is easily understood from Equation 8c. Thus, to explain the dependence on purity from melt to melt, one is

forced to accept the finite impurity source present in the melt model as being dominant over the infinite impurity source model (source from reaction with the reactor walls).

7.2 OPTIMUM GROWTH PARAMETERS

Recogniton that the finite impurity source of the indium melt dominates impurity incorporation for the 750°C source suggests that improved purity may be obtained if the concentration of the impurity in the melt could be reduced. Unfortunately, any reaction which would transport the impurity away from the melt while in the reactor would also transport indium. Therefore, it is desirable to find a set of growth parameters which would support a very high impurity transport rate while supporting only a low indium transport rate. It was found that with the 700°C indium source temperature, the relative growth rate and impurity incorporation rate could be adjusted so that the impurity transport rate was lowered at low mole fractions of PCl_3 and greatly increased for higher mole fraction. Under the conditions of low mole fraction a slow melt clean-up was evidenced by gradual increase in mobility and decrease in carrier concentration. More radical evidence of melt purification inside the reactor is obtained from the growth runs in which the growth run performed at a low mole fraction with the original concentration of impurity was reproduced

in one of the later growth runs on the same melt after several intermediate growth runs were performed at a high mole fraction. For all melts tested in this way, the later run proved to be much purer than the original run it duplicated.

7.3 REACTING SPECIES IDENTIFICATION

For reasons already discussed in the development of the incorporation model, it is not possible to know exactly what reactions occur and which reaction mechanisms are responsible for the transport of the impurity and purification of the melt. Appealing to equilibrium considerations, one can obtain some qualitative indication of a possible mechanism or mechanisms. Figures 24 and 25 [16] show the dependence of equilibrium partial pressures on source temperatures for a constant mole fraction of PCl_3 and the dependence of equilibrium partial pressures on PCl_3 mole fraction for a source temperature of 750°C, respectively, above the solid InP surface of the melt.

Of course, these values are not the actual values obtained in the reactor but they are useful in indicating general trends and relationships between the chemical species present. Referring to Figure 24 one observes that for a change in source temperature from 700°C to 750°C the only species which change appreciably are HCl and P_2 (both change by about a factor of 2). Because

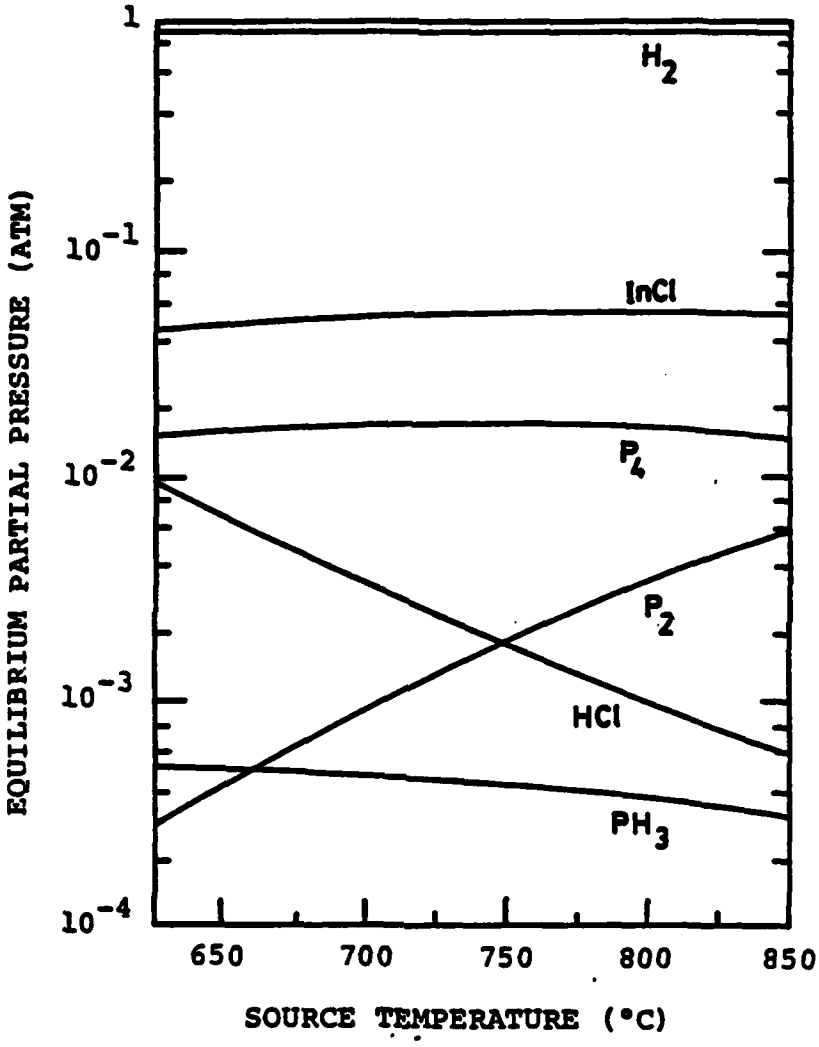

Figure 23 Equilibrium partial pressures as a function of source temperature for 2×10^{-2} atm PCl_3 partial pressure.

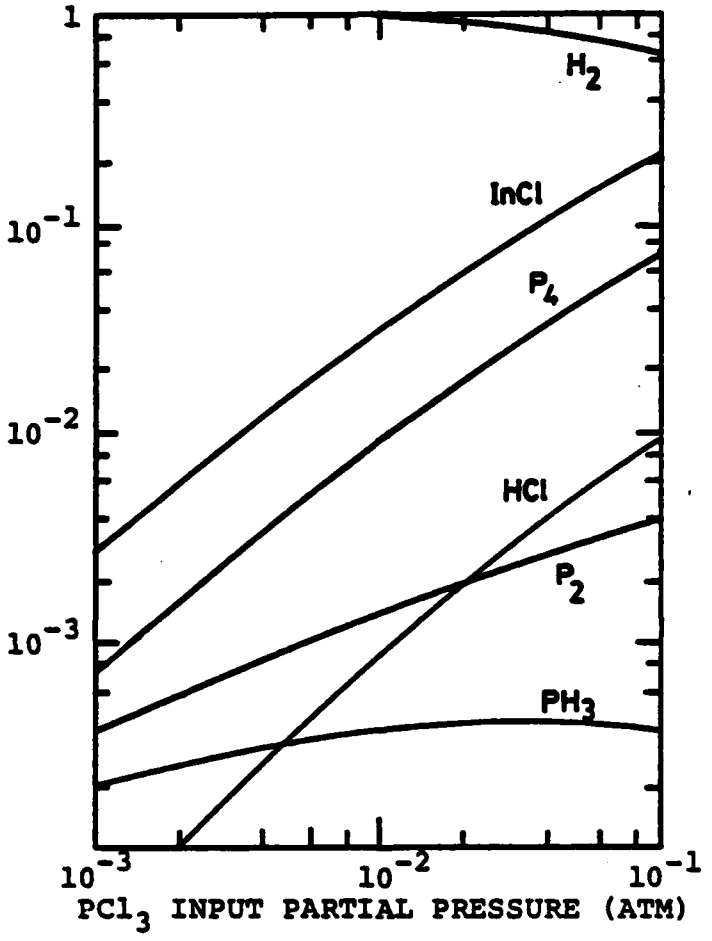

Figure 24 Equilibrium partial pressures at 750°c as a function of PCl_3 partial pressure.

the mole fraction effect is due (at least in part) to the flux of impurities down the reaction tube, it is reasonable to believe that, for the reactor operating in this temperature range, either HCl or P_2 is associated with the reaction with the impurity. This belief is further supported from the PCl_3 mole fraction dependence of equilibrium partial pressures in Figure 25. For PCl_3 mole fractions of from 2% to 4% one sees a great change in the stoichiometry of the gas stream above the melt with the greatest change occurring with the HCl (factor of 5 change).

Recapitulating, IMPINC was used to determine a general, qualitative indication that there exists in the melt an impurity which is greatly responsible for the doping of the melt. Two possibilities for the identity of the chemical species in the gas stream responsible for the transport of impurities are P_2 and HCl. Using the above information it was possible to adjust the growth parameters to achieve higher purity samples.

There was observed a dependence of purity on the PCl_3 input mole fraction when the 700 °C source temperature profile was used. Also associated with growth runs performed with the 700 °C source temperature was the apparent purification of the indium source evidenced by

the gradual increase in the purity of the samples grown with successive growth runs performed on a melt.

Experiments were performed to determine the effect of varying the PCl_3 mole fraction during the lifetime of a melt. The saturation and first growth run on the melt were performed at a low mole fraction and the mole fraction was increased with each successive growth run. For the final growth runs performed on the melt, the PCl_3 mole fraction was returned to the low mole fraction of the original growth run. With the return of the mole fraction to its original level, there appeared a large increase in the purity of the material over the first run on the melt. This was taken as being further evidence of *in situ* melt purification. The results of growth runs performed with the 700°C source temperature profile are set forth in Table 7.

8. CONCLUSIONS

The literature reports that many researchers have observed a distinct mole fraction effect in the growth of InP. The actual mechanism through which the molar fraction of PCl_3 injected into the reaction vessel controls incorporation of impurities into the growing InP layer is not clear and is further obscured by the dependence of purity upon the physical design of the reactor. The model for impurity transport/incorporation developed by DiLorenzo and Moore [16] to explain the dependence of GaAs growth on $AlCl_3$ mole fraction may be used, in a general way, to explain the PCl_3 mole fraction dependence of impurity incorporation in InP growth [5]. In addition to the transport of impurities, there is also the mechanism of incorporation of the impurity (if indeed what is being observed is impurity incorporation) into the growing layer which is dependent upon the thermodynamic properties of the reactions which occur at the surface of the growing layer and the non-equilibrium kinetics of the same reactions. Any change in the mole fraction would alter the partial pressure of the reacting chemical species along the length of the reaction tube as well as at the surface of the reaction. This coupled dependence on transport and incorporation raises the question of which mechanism impurity flux or surface

reactions ultimately dominates in controlling the purity of the grown layers. It has been shown that using the model developed in this paper augmented with results obtained from actual growth runs performed in Reactor D for a wide range of growth parameters, a qualitative understanding of the effects which control the purity of the grown layer may be obtained which successfully explains the behavior of the reactor. Using this understanding led to the adjustment of the growth parameters to achieve conditions in the reactor which yielded higher purity material while demonstrating a marked dependence of PCl_3 mole fraction on purity. Using this data to supplement what had already been discovered about the system indicated that the impurity which was being incorporated into the epitaxial layer was associated with transport of the impurity from a finite source resident in the indium melt.

The source temperature dependence of the mole fraction effect used in conjunction with the equilibrium partial pressures of the species present in the gas stream above the solid InP crust of the melt gave two possibilities for the constituants of the gas stream which take part in the impurity transport reaction - HCl and P_2. It must be stressed that these choices only represent a possibility for the species involved in the transport reaction.

Recognition that the impurity associated with the indium melt was finite gave rise to the possibility that the melt could be purified through the proper choice of growth parameters prior to growth runs being performed. Indeed, experiments performed did indicate that considerable melt clean-up could be achieved by running the reactor through several growth cycles with an elevated PCl_3 mole fraction.

In summary, it has been shown that higher purity material may be achieved using lower reactor temperatures with the PCl_3 mole fraction effect to reduce the rate of impurity transport from the melt. The concentration of the impurity in the melt may be reduced to give even higher purity at the expense of shorter melt lifetimes by increasing the rate of impurity transport down the reaction tube prior to any growth run.

9. BIBLIOGRAPHY

1. R.C. Clarke and L.L. Taylor, "The Preparation of High-Purity Epitaxial InP", *Solid State Communications* 8, 1125, (1970).

2. R.C. Clarke and L.L. Taylor, "Pure and Doped Indium Phosphide by VPE", *Journal of Crystal Growth* 43, 473, (1978).

3. R.C. Clarke, "Chemistry of the In-H_2-PCl_3 Process", *Gallium Arsenide and Related Compounds* 45, Institute of Physics Conference Series, 19, (1978).

4. R.C. Clarke and L.L. Taylor, "Multilayer Structures of Epitaxial InP", *Journal of Crystal Growth* 31, 190, (1975).

5. M.C. Hales and J.R. Knight, "The Electrical Properties of Vapor Epitaxial Indium Phosphide Grown in the Presence of Oxygen", *Journal of Crystal Growth* 46, 582, (1979).

6. R.D. Fairman, M. Omori, and F.B. Fank, "Recent Progress in the Control of High-Purity VPE InP by the $PCl_3/In/H_2$ Technique", *Gallium Arsenide and Related Compounds* 33b, 45, (1976).

7. J.V. DiLorenzo and G.E. Moore, Jr., "Effects of $AsCl_3$ Mole Fraction on the Incorporation of Germanium, Silicon, Selenium, and Sulfur into Vapor Grown Epitaxial Layers of GaAs", *Journal of the Electrochemical Society* 118, No. 11, 1823, (1971).

8. C.D. Hodgman, *Handbook of Chemistry and Physics*, The Chemical Rubber Publishing Co., Cleveland, Ohio, 2437, (1963).

9. A.R. Clawson, "Laboratory Procedures for Etching and Polishing InP Semiconductors", *NOSC Technical Note 592*, (December, 1978).

10. R.N. Hall, "Solubility of III-V Compound Semiconductors in Column III Liquids", *Journal of the Electrochemical Society* 110, No. 5, 385, (1963).

11. L.J. Van der Pauw, "A Method of Measuring Resistivity and Hall Effect of Discs of Arbitrary Shape", *Philips Research Reports* 13, 111, (1958).

12. L.J. Van der Pauw, "A Method of Measuring Lamellae of Arbitrary Shape", *Philips Technical Review* 20, 220, (1958).

13. O. Lindberg, "Hall Effect", *Proceedings of the IRE* 40, No. 11, 1414, (1952).

14. G.E. Stillman and C.M. Wolfe, "Electrical Characterization of Epitaxial Layers", *Thin Solid Films* 31, 69, (1976).

15. T.B. Reed, "Free Energy of Formation of Binary Compounds", MIT Press, Cambridge, MA., (1971).

16. D.W. Shaw, "A Comparative Thermodynamic Analysis of InP and GaAs Deposition", *Journal of Physics Chemical Solids* 36, 111, (1975).

17. O. Levenspiel, "Chemical Reaction Engineering", John Wiley and Sons, NY, NY, (1972).

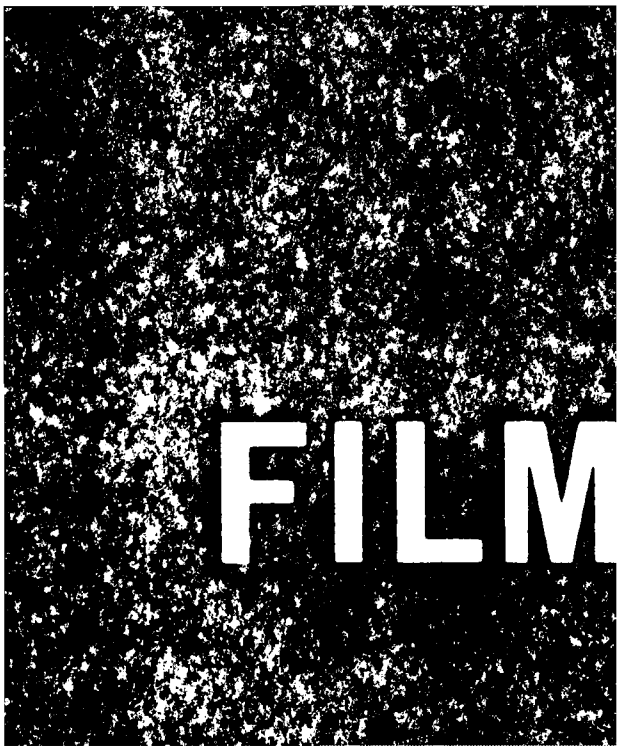
FILM